

1 **Seabed morphology and sedimentary processes on high-gradient trough mouth fans**
2 **offshore Troms, northern Norway**

3

4 Tom Arne Rydningen^{a,b*}, Jan Sverre Laberg^a, Vidar Kolstad^b

5 ^aDepartment of Geology, University of Tromsø – The Arctic University of Norway, N-9037 Tromsø, Norway

6 ^bDONG E&P Norge AS, Roald Amundsens Plass 1, N-9257 Tromsø, Norway

7 *Corresponding author: Tom Arne Rydningen, e-mail: tom.a.rydningen@uit.no

8

9 **Abstract**

10 Trough mouth fans (TMF) situated at the mouths of formerly glaciated cross-shelf troughs are
11 important palaeoclimatic archives. Whereas the sedimentary processes of large, low-gradient
12 TMFs have received considerable interest, little attention has been paid to the other end
13 member of this landform class, i.e. TMFs with higher slope gradients. Detailed swath-
14 bathymetric data and seismic profiles from the continental margin offshore Troms, northern
15 Norway cover three high-gradient TMFs (the Andfjorden, Malangsdjupet and Rebbenisdjupet
16 TMFs; slope gradients generally between 1° and 15°), as well as inter-fan areas, which
17 include two submarine canyons (the Andøya and Senja Canyon) and the Malangsgrunnen
18 inter-fan slope. The present-day morphologies of the Andfjorden and Malangsdjupet TMFs
19 have evolved from sediment transport and distribution through gully-channel complexes. The
20 Andfjorden TMF has later been affected by a large submarine landslide that remobilized
21 much of these complexes. The Rebbenisdjupet TMF is dominated by a number of small and
22 relatively shallow slide scars, which are inferred to be related to small-scale sediment failure
23 of glaciomarine and/or contouritic sediments. The canyons cut into the adjacent TMFs, and
24 turbidity currents originating on the fans widened and deepened the canyons during
25 downslope flow. The Malangsgrunnen shelf break and inter-fan slope acted as a funnel for
26 turbidity currents originating on the upper slope, forming a dendritic pattern of gullies. A
27 conceptual model for the high-gradient TMFs on the Troms margin has been compiled. The
28 main sediment input onto the TMFs has occurred during peak glacials when the
29 Fennoscandian Ice Sheet reached the shelf edge. The overall convex fan form and
30 progradational seismic facies show that these glacial deposits were repeatedly distributed
31 onto the fan. On the Andfjorden and Malangsdjupet TMFs, gully-channel complexes occur
32 within such deposits. It is thus inferred that the steep slope of these TMFs promoted rapid
33 transformation from small-scale slumps and debris flows on the upper slope, into partly

34 erosive turbidity currents. These flows continued into the deep sea, thus promoting efficient
35 sediment by-pass across the TMFs. This model can be applied to other TMFs situated at the
36 mouths of other glaciated cross-shelf troughs. In contrast, low-gradient TMFs are found to be
37 dominated by glaciogenic debris flow deposits. Furthermore, gully-channels complexes
38 demonstrating the presence of erosive turbidity currents on high-gradient TMFs are rare on
39 low-gradient TMFs. Large submarine landslides occur at both high- and low-gradient TMFs.

40

41 **Keywords:** high-gradient trough mouth fans, gully, canyon, continental slope, submarine
42 landslide, Troms

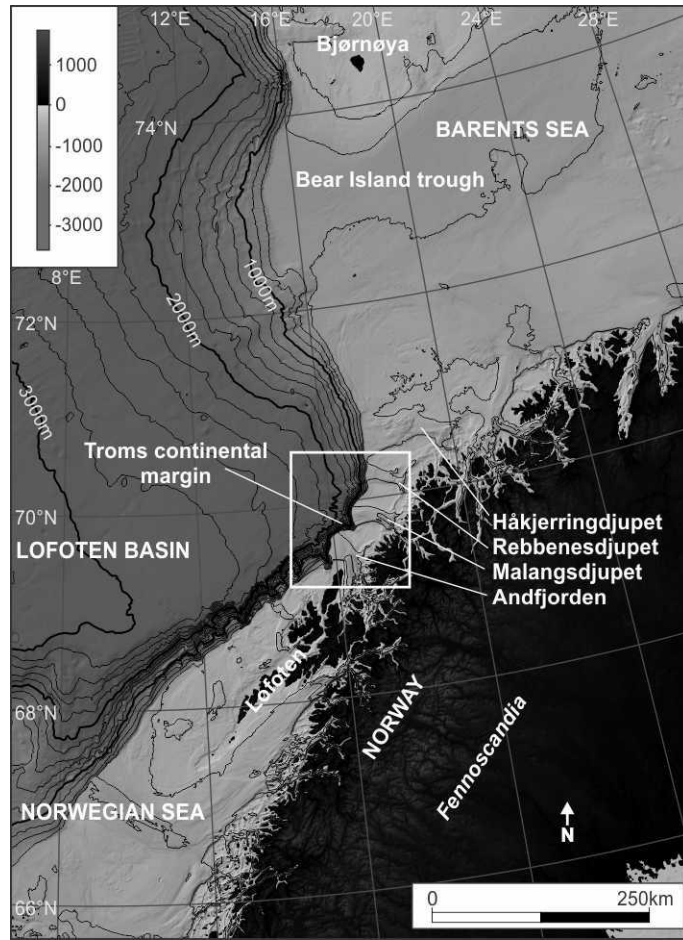
43 **1 Introduction**

44 Trough mouth fans (TMF) are confined depocentres of glacial sediments located at the
45 mouth of transverse troughs on glaciated continental margins (Vorren et al., 1989; Vorren and
46 Laberg, 1997). The TMFs have developed over successive late Cenozoic glacial-interglacial
47 cycles by the delivery of large volumes of subglacial sediment to the termini of ice streams
48 flowing along troughs, and subsequent re-deposition down the continental slope via
49 massflows. TMFs therefore represent important palaeoclimatic archives in both northern and
50 southern high-latitudes (Vorren and Laberg, 1997; Clausen, 1998; Dahlgren et al., 2005;
51 Sejrup et al., 2005; Rebesco et al., 2006; Dowdeswell et al., 2008). Erosion and transport of
52 glacial sediments to the margin was mainly achieved by fast-flowing ice streams overlying
53 transverse shelf troughs during glacial maxima (Laberg and Vorren, 1995; 1996a; b; King et
54 al., 1996; Vorren and Laberg, 1997; Dahlgren et al., 2005; Laberg et al., 2012). Conversely,
55 when the ice retreated the sedimentation was focused on the inner shelves and fjords (Vorren
56 et al., 1989; Sejrup et al., 1996). Inter-fan areas were generally sediment-starved during peak
57 glaciations (Vanneste et al., 2007).

58 In general, the studied TMFs on the Norwegian margin are low-gradient features with angle
59 of dip usually between 0.5 and 1°, e.g. the North Sea TMF and the Bear Island TMF (Vorren
60 and Laberg, 1997). The main morphological elements of these TMFs are glacial debris
61 flow (GDF) debrites (Vogt et al., 1993; Laberg and Vorren, 1995; King et al., 1996; Vorren
62 and Laberg, 1997). Individual GDF debrites vary between 1 and 40 km in width, 5 and 60 m
63 in thickness, and stretches 10 to more than 200 km into the deep sea (King et al., 1996;
64 Vorren and Laberg, 1997). These have a lithology similar to their source, i.e. they comprise
65 glacial diamicton derived from the shelf (e.g. Laberg and Vorren, 1995). The deposits were
66 subsequently affected by sediment remobilization from major submarine landslides (Laberg
67 and Vorren, 1993; 2000; Laberg et al., 2000; Haflidason et al., 2004; Bryn et al., 2005;

68 Hjelstuen et al, 2007) and gully-forming erosional currents (Vorren et al., 1989; Laberg and
69 Vorren, 1995).

70 Whereas the surface morphology of the large and low-gradient TMFs have received
71 considerable interest, little attention has so far been paid to the other end member of this
72 landform class, i.e. TMFs holding a high slope gradient ($>4^\circ$) (Ó Cofaigh et al., 2003;
73 Batchelor and Dowdeswell, 2014), here termed high-gradient TMFs. In this study, multi-beam
74 swath-bathymetric data sets are combined with 2D multi-channel seismic lines in order to
75 investigate the seabed geomorphology of the continental slope off Troms, northern Norway
76 (Fig. 1), which is comprised of three high-gradient TMFs with slope gradients generally
77 varying between 1° and 15° ; the Andfjorden, Malangsdjupet, and Rebbenisdjupet TMFs (Fig.
78 2). These high-gradient TMFs were fed by palaeo-ice streams which were active during
79 glacial maxima including the LGM (the Last Glacial Maximum) (Ottesen et al., 2005; 2008;
80 Rydningen et al., 2013, submitted), similar to their low-gradient counterparts both on the
81 Norwegian margin (e.g. Vorren and Laberg, 1997) and on other glaciated margins (e.g. Aksu
82 and Hiscott, 1992; Rebesco et al., 2006; Laberg et al., 2013). The aims of this study are to: 1)
83 describe and discuss the seafloor morphology of the high-gradient TMFs, 2) identify the main
84 sedimentary processes responsible for the formation of the recentmost part of these fans, and
85 3) compare and contrast the processes on high- and low-gradient TMFs.

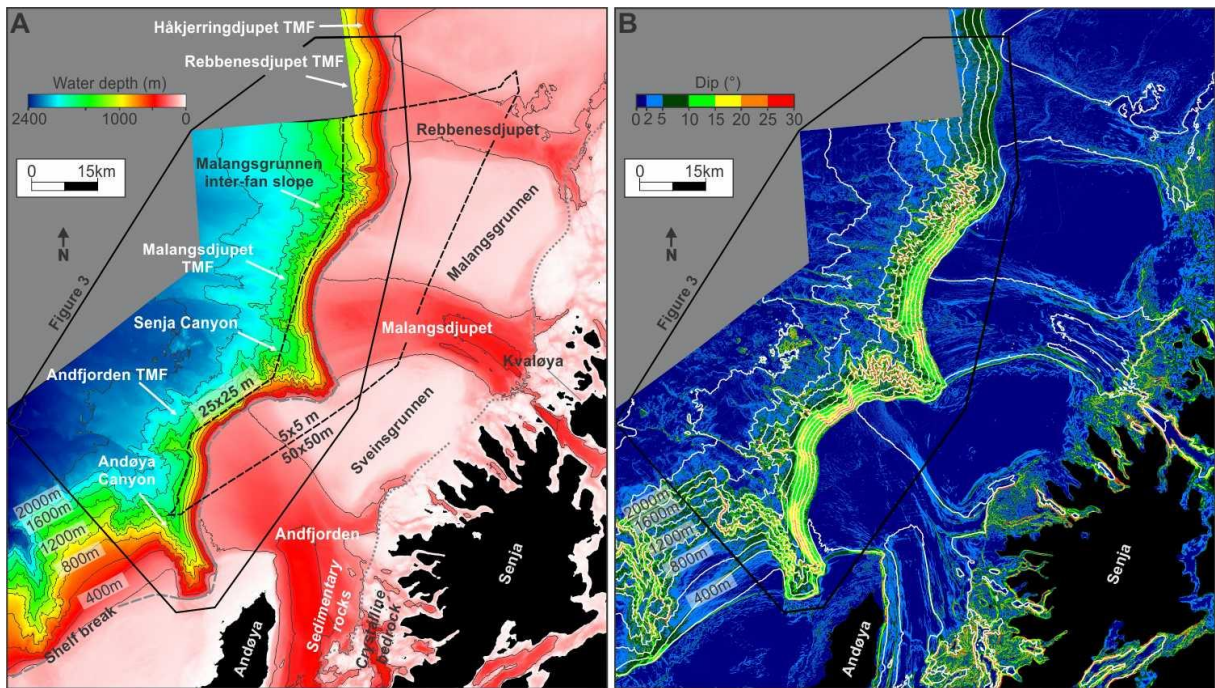


86

87 **Fig. 1: Bathymetric map of the Norwegian Sea and the SW Barents Sea generated from the IBCAO**
 88 **database (Jakobsson et al., 2012). Contour interval is 200 m. The study area is indicated by the white box.**

89 **2 Physiographic and geologic setting**

90 The present continental shelf off Troms is characterized by three deep cross-shelf troughs,
 91 Andfjorden, Malangsdjupet, and Rebbenesdjupet, which are separated by the shallow banks
 92 of Sveinsgrunnen and Malanggrunnen (Fig. 2). The shelf break is situated at 100 to 300 m
 93 water depth and is located 30 to 60 km west of the islands of Senja and Kvaløya, respectively,
 94 and 10 km west of Andøya (Fig. 2). The continental slope is dominated by the Andfjorden,
 95 Malangsdjupet and Rebbenesdjupet TMFs. The fans are separated by inter-fan areas including
 96 two canyons, the Andøya and Senja canyons, and the slope west of the Malanggrunnen bank
 97 (Fig. 2).



98

99 **Fig. 2: The area of study. A: Bathymetric map of the continental shelf and slope outside Troms County,**
 100 **northern Norway. The dashed lines delimit data sets with different spatial resolution. B: Dip map of the**
 101 **seabed.**

102 The 40 km long Andøya Canyon cuts into the slope and outer shelf west of the island of
 103 Andøya (Fig. 2). The width between the canyon shoulders is ~9 km, and the maximum
 104 incision is 1100 m (Laberg et al., 2007). The western sidewall of the canyon consists of drift
 105 sediments modified by sliding and slumping. Infilling of glacial sediments by the
 106 Andfjorden TMF make up the steep (20-25°) eastern sidewall, where gullies are frequent.
 107 Axial incision is inferred to be due to erosion by turbidity currents originating from the
 108 downslope flow of both glacial and drift sediments (Laberg et al., 2007).

109 The Andfjorden TMF has been partly affected by the Andøya Slide. Based on GLORIA long-
 110 range side-scan sonar data this slide was initially believed to cover an area of 9,700 km²
 111 (Dowdeswell et al., 1996; Laberg et al., 2000). Later, Rise et al. (2009), based on high-
 112 resolution swath-bathymetric data, restricted the extent of the slide affected area which was
 113 shown to include several larger and smaller slides.

114 Regional mapping of surface sediments and landforms on the continental slope offshore
115 northern Norway has been carried out by Bugge (1983), Kenyon (1987), Taylor et al. (2000),
116 and the Mareano program (www.mareano.no). The shelf is covered with up to 200 m of
117 Quaternary sediments (Rydningen et al., submitted), consisting mainly of till, glaciomarine
118 silt and clay, as well as iceberg turbate (Vorren et al., 1988; Vorren and Plassen, 2002; Bellec
119 et al., 2009). Pronounced depocentres of glacial sediments, reaching over 1 km in
120 thickness, are located at the trough mouths, forming the TMFs (Oljedirektoratet, 2010;
121 Rydningen et al., submitted). They document focused glacial erosion of the shelf throughout
122 the Quaternary (Dahlgren et al., 2005; Rydningen et al., submitted). Down to a water depth of
123 about 1200 to 1500 m, sandy gravel, gravelly sand and muddy/sandy gravel dominate, while
124 the deeper parts of the slope consist of mud and blocks/areas of stiffer sediments (Bellec et
125 al., 2012a: b).

126 The Fennoscandian Ice Sheet advanced across the continental shelf off Troms twice during
127 the last ~26 ka cal BP (Vorren and Plassen, 2002; Vorren et al., 2015). Fast-flowing ice
128 streams carved out the cross-shelf troughs as they flowed towards the shelf break, while
129 sluggish-flowing ice was situated on the banks (Ottesen et al., 2008; Rydningen et al., 2013).
130 The deglaciation of the shelf was stepwise; the initial breakup of the ice started at the trough
131 mouths, while the ice remained grounded on the banks. Most of the shelf was ice-free at 17.5
132 ka cal BP (Rydningen et al., 2013; Vorren et al., 2015).

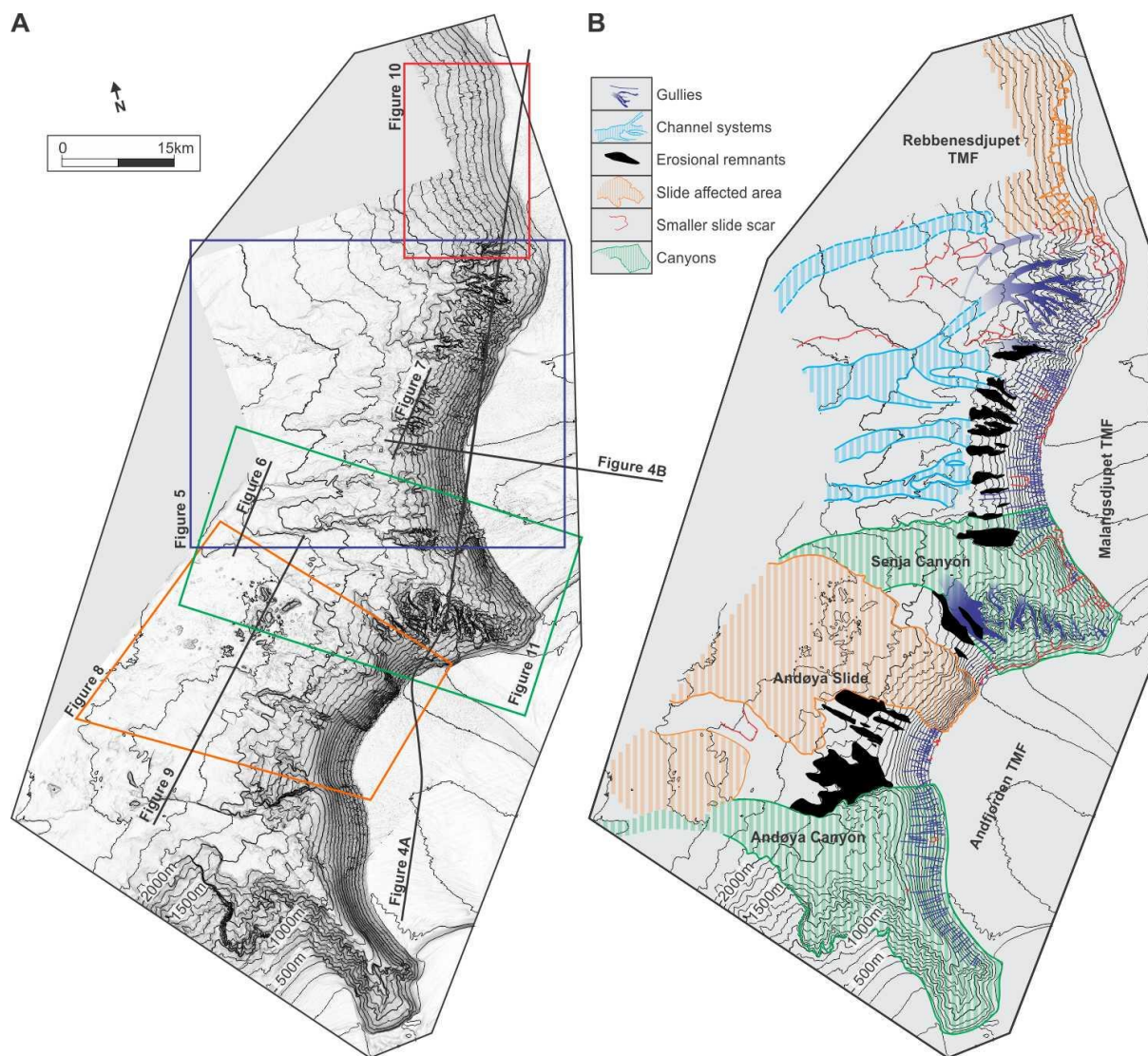
133 The present oceanography of the area is influenced by three major water masses. The
134 Norwegian Coastal Current is transporting low-salinity water with variable temperature
135 northwards near the coast. This water overlies the relatively warm and saline Norwegian
136 Atlantic Current, which extends down to between 500 and 600 m within the study area. This
137 current splits in two branches; one part branches off to the southern Barents Sea, whereas the
138 other branch continues northwards along the Barents Sea slope (Hansen and Østerhus, 2000;

139 Ślobowska-Woldengen et al., 2008). Below the Norwegian Atlantic Current, two cold-water
140 masses are present: the Norwegian Sea Arctic Intermediate Water and the Norwegian Sea
141 Deep Water. The border between these two water masses occurs typically at around 1000 m
142 water depth (Buhl-Mortensen et al., 2012).

143 **3 Data and methods**

144 The data sets used in this study consist of swath-bathymetric data and commercial 2D-seismic
145 lines. The Norwegian Hydrographic Service collected the swath-bathymetric data between
146 1990 and 2004 using Simrad EM100 and EM1002 multi-beam echo-sounders, and the data
147 sets were provided to the University of Tromsø through the Norway Digital initiative. The
148 data sets are available as UTM-points with 50x50 m horizontal spacing within 12 nautical
149 miles from the shoreline. Further seawards, the data sets are available as 5x5 m points down
150 to approximately 1000-1400 m water depth, and as 25x25 m points beyond this. The
151 bathymetric data sets cover the Andfjorden and Malangsdjupet TMFs down to ~2400 m water
152 depth, as well as the southern half of the Rebbenedjupet TMF down to ~2100 m (Fig. 2). The
153 gridding and visualization were done in ED50 UTM zone 32N using the Global Mapper® and
154 Petrel® software. From these data sets, slope maps (e.g. Fig. 2B and 3A) and slope direction
155 maps were generated. Parallel ship track lines and other artefacts were noted to avoid
156 misinterpretations.

157 The upper sections of seismic lines from the Norwegian Petroleum Directorate, acquired
158 between 2007 and 2009, were made available for this study. The seismic lines were visualized
159 and analyzed in the Petrel® software of Schlumberger.



160

161 **Fig. 3: The outer continental shelf and upper slope off northern Norway. See Fig. 2 for location. A: Slope**
 162 **gradient map. Areas of steep slopes have a darker colour. Locations of detail figures and seismic lines are**
 163 **indicated. B: Interpretation of landforms discussed in this paper. TMF=Trough Mouth Fan.**

164

165 **4 Results**

166 The late Cenozoic seismic stratigraphy of the Troms continental margin is detailed in
167 Rydningen et al. (submitted), and summarized below. Following this, the slope gradient and
168 morphology of the three TMFs and inter-fan areas are presented (Fig. 3; also summarized in
169 Table 1).

170 **4.1 Seismic stratigraphy**

171 The middle and outer shelf comprises late Cenozoic sediments which are subdivided into four
172 seismic units: S1 (oldest) to S4, bounded by four regional horizons (T1-T4; Fig. 4A and B).

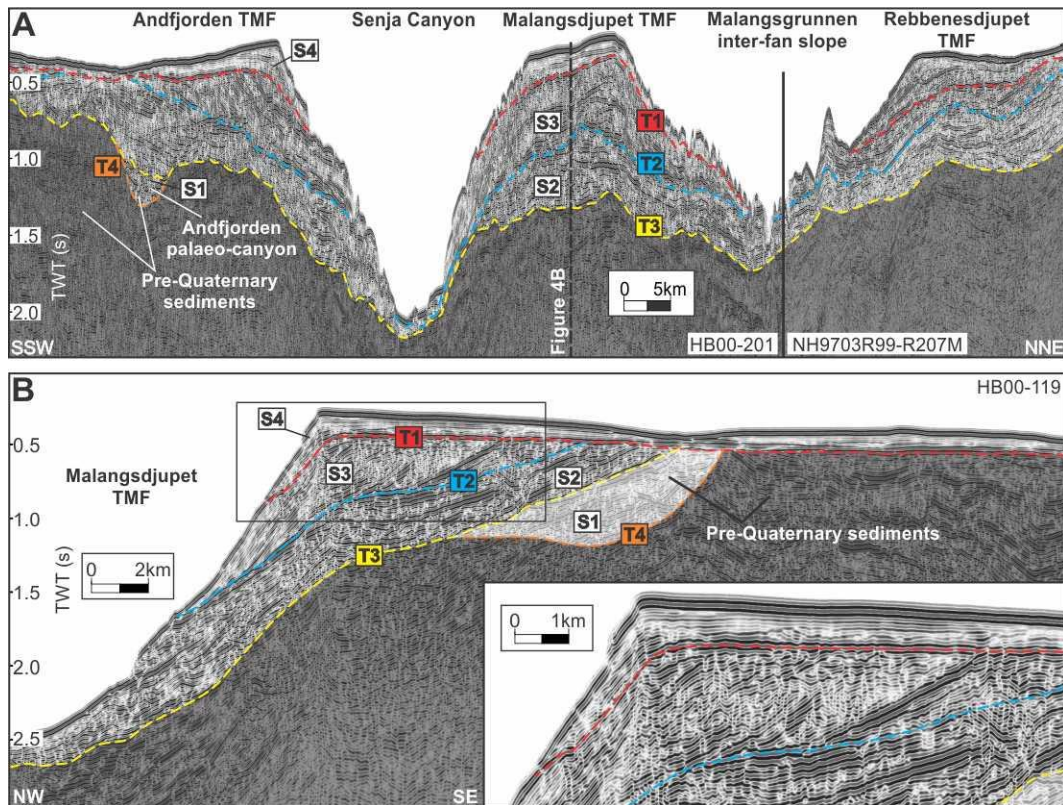
173 Unit S1 is inferred to be of pre-Quaternary age and is completely buried by units S2-S4
174 (Rydningen et al., submitted).

175 Unit S2 comprises stacked, sub-parallel seaward-dipping clinoforms, interpreted to be
176 dominated by suspension fallout and turbidity currents. Glaciomarine and glaciofluvial
177 conditions prevailed during deposition of unit S2, which commenced at ~2.7 Ma (Rydningen
178 et al., submitted). This unit outcrops on the lower slope of the Andfjorden and Malangsdjupet
179 TMFs, at a water depth of ~1200 m (Fig. 4B).

180 Unit S3 comprises clinoforms with a steeper gradient, which are interpreted to mark a shift
181 towards more intensified glaciations, including repeated advances of fast-flowing ice streams
182 across the shelf, depositing subglacial deformation till at the shelf break. Later, these deposits
183 were reworked by debris flows and turbidity currents and deposited on the slope (Rydningen
184 et al., submitted). Together with unit S4, this unit makes up the present-day morphology of
185 the Andfjorden and Malangsdjupet TMFs down to where unit S2 outcrops.

186 Unit S4 is a sheet-like deposit which covers the shelf and upper slopes of the Andfjorden and
187 Malangsdjupet TMFs, as well as the entire Rebbenisdjupet TMF. The internal acoustic
188 reflection configuration of the unit on the shelf is aggrading, with several internal

189 unconformities which show evidence of former fast-flowing ice streams traversing the cross-
 190 shelf troughs. Thus, unit S4 also comprises subglacial deformation till (Rydningen et al.,
 191 submitted). Below, we focus on the sea-floor morphology which represents the upper part of
 192 seismic unit S4 on the shelf and upper slope, and the outcropping units S3 and S2 on the
 193 lower slope (Fig. 4B).



194

195 **Fig. 4: Seismo-stratigraphic framework of the late Cenozoic sediments on the Troms margin (adopted**
 196 **from Rydningen et al., submitted). See Fig. 3 for location of profiles. A: Composite seismic strike line**
 197 **crossing the study area. B: Seismic dip line crossing the shelf break in the Malangsdjupet trough.**

198 4.2 Continental slope gradient

199 From the convex-shaped shelf break to a water depth of ~1400 m, both the Andfjorden and
 200 Malangsdjupet TMFs are characterized by slope angles between 10° and 15° (Fig. 2B). Areas
 201 of highest gradient (~15° to ~35°) are associated with escarpments due to sliding/slumping
 202 and gravity flow erosion. At ~1400 m water depth a marked reduction in slope gradient

203 occurs; between 1400 and 1600 m water depth the gradient of both fans is between 5° and
204 10°, before it decreases to below 5° between 1600 and 2000 m (Fig. 2B). From ~2000 m
205 water depth the slope gradient is below 2° (Fig. 2B).

206 The Rebbenedjupet TMF is generally characterized by a lower slope gradient. Similar to the
207 other TMFs, this fan is steepest in the upper reaches, with gradients between 5° and 8° down
208 to a water depth of 1200 m. Further downslope the gradient decreases to below 2°. Unlike the
209 other TMFs, the gradient decreases more gradually seaward, i.e. this TMF has no pronounced
210 circumference in its upper part (Fig. 2). The northern part of the Rebbenedjupet TMF is
211 coterminous with the southern part of the Håkjerringdjupet TMF (Fig. 1 and 2).

212 These TMFs have the steepest gradient reported from the Norwegian – Barents Sea –
213 Svalbard continental margin and their gradients are comparable to TMFs and prograding
214 wedges offshore the Antarctic Peninsula (Larter and Cunningham, 1993; Dowdeswell et al.,
215 2004; Amblas et al., 2006), Greenland (Clausen, 1998; Nielsen et al., 2005; García et al.,
216 2012), as well as the eastern Canadian margin (Batchelor and Dowdeswell, 2014).

217 **4.3 Trough Mouth Fan morphology**

218 4.3.1 Gully-channel complexes

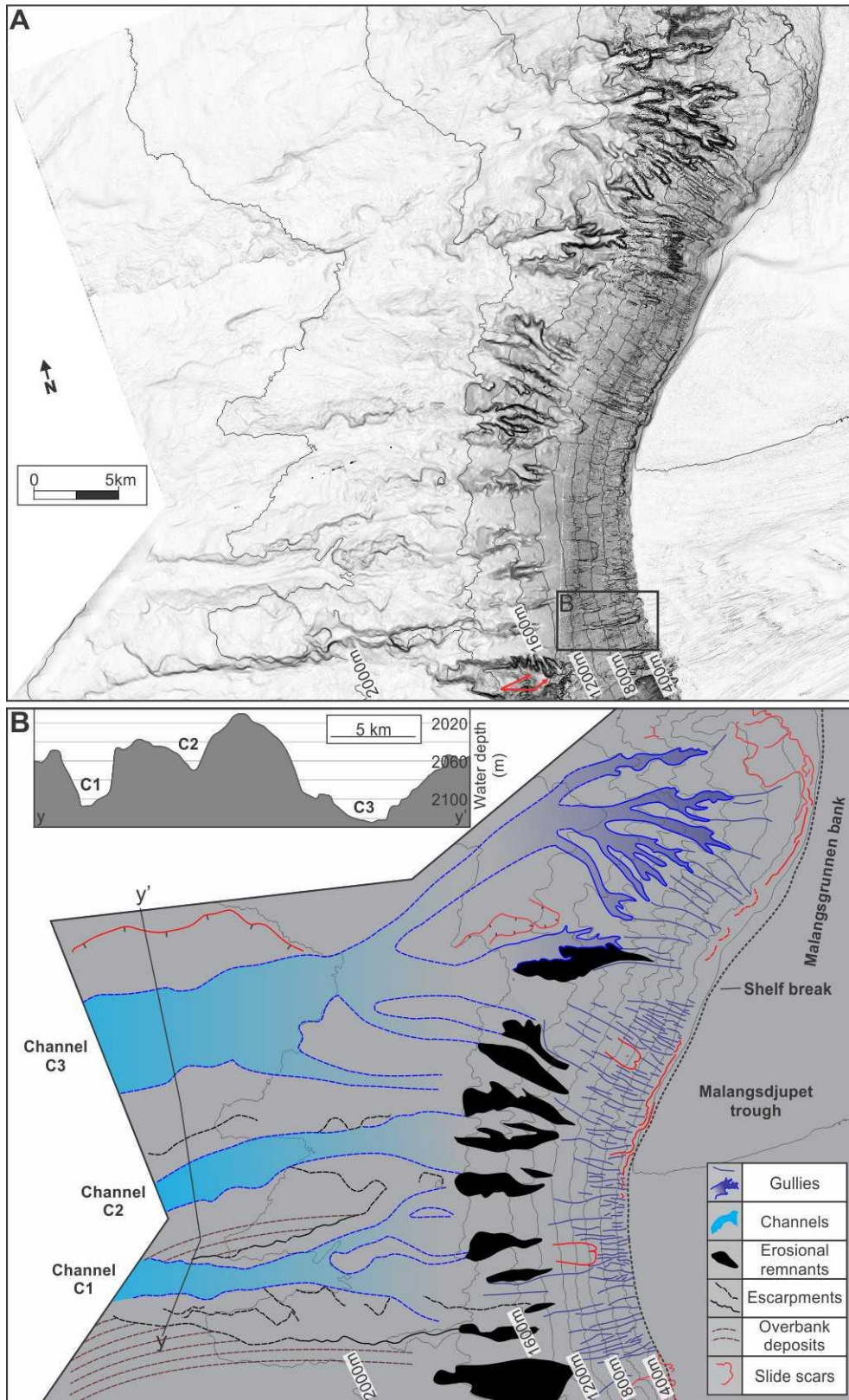
219 The upper, steepest part of the Andfjorden and Malangsdjupet TMFs are dominated by a
220 number of straight to slightly curved gullies (Fig. 3 and 5) which are relatively deep (5 to 50
221 m) compared with their width (100 to 500 m). Gullies both originate at the shelf break as
222 small slide scars, some of which are partly buried in their upper reaches (see Fig. 12 in Laberg
223 et al., 2007), and as single furrows between 100 and 200 m downslope of the shelf break. No
224 connection to channels on the shelf has been observed.

225 The gullies represent the upper part of a gully-channel complex which dominates the
226 morphology on the Malangsdjupet TMF (Fig. 5). Part of a similar system is located on the

227 Andfjorden TMF between the Andøya Slide and the Andøya Canyon (Fig. 3). The gullies
228 show a dispersing character on the upper part of the complexes, probably due to the convex-
229 shaped shelf break. The upper gully-dominated part can be followed to a water depth of
230 ~1200 m, where downslope oriented and high-relief ridges occur (Fig. 5; see below). On the
231 Malangsdjupet TMF the gullies from this depth merge into channels, which are distinguished
232 from gullies in being wider (1 to 6 km). The channels are coalescing further downslope into
233 three main channels (C1, C2 and C3) from a water depth of ~1800 m (Fig. 5). This is inferred
234 to be controlled by the distribution and location of the high-relief ridges focusing the flows
235 into the inter-ridge areas and channels. A cut-and-fill pattern is inferred from a seismic profile
236 crossing the lower part of the channels (Fig. 6) showing lateral channel migration.

237 Based on a comparative study of gullies on Arctic and Antarctic margins, Gales et al. (2013)
238 concluded that gullies likely evolve through either downslope erosion by turbidity currents,
239 which may be initiated by discharges of sediment-laden subglacial meltwater, or through
240 headward erosion by retrogressive mass failures, which may occur both during glacial and
241 interglacials. Many of the straight gullies on the Troms margin are partly infilled on the upper
242 parts of the TMFs. This most likely took place through the deposition of subglacial sediments
243 during the LGM, and not during the present interglacial when the northward flowing
244 Norwegian Current is erosive to a water depth between 500 and 600 m, below the shelf break.
245 The fresh-looking gullies that are not infilled and thus are younger formed after the onset of
246 ice recession, i.e. during the Holocene.

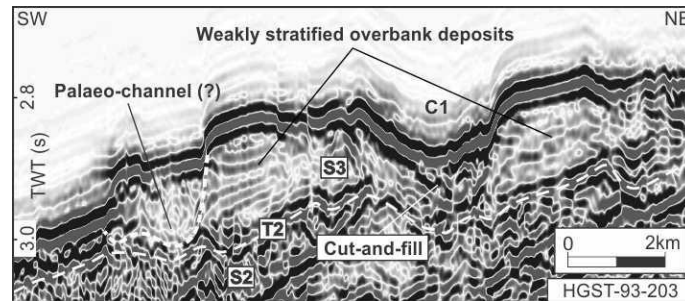
247 Based on the data at hand it is difficult to discriminate between an origin from erosion by
248 sediment-laden bottom currents derived from a shelf break-terminating ice sheet, or small
249 scale sediment failure during LGM for the partly buried gullies. For the Holocene gullies, an
250 origin from sediment failure is favoured, since no indications of cold bottom-water formation
251 in the troughs during the present interglacial have been reported.



252

253 **Fig. 5: The Malangsdjupet Trough Mouth Fan and the Malangsrunden inter-fan slope. See Fig. 3 for**
 254 **location. A: Slope gradient map. Red arrows indicate slide scars on erosional remnants. B: Interpretation**
 255 **of A. Gullies dominate the Trough Mouth Fan morphology down to 1200 m water depth, before they**

256 merge into channels on the lower slope (C1, C2 and C3). The depths of the channels are illustrated by a
257 bathymetric profile. The Malangsrunden inter-fan slope is dominated by slides and gullies forming a
258 dendritic pattern merging into C3 on the lower slope.

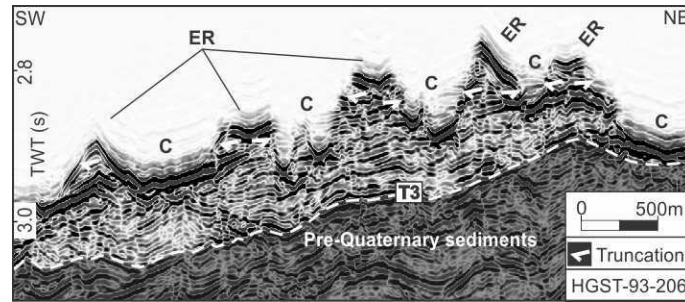


259

260 **Fig. 6: Seismic profile across overbank deposits showing a weak internal stratification. Channel C1 erodes**
261 **into the overbank deposit and has a cut-and-fill character. A possible palaeo-channel is located in the**
262 **northern part of the Senja Canyon channel. See Fig. 3 for location.**

263 4.3.2 Downslope-oriented ridges – erosional remnants

264 Distinct linear, high-relief ridges are found on the Andfjorden and Malangsdjupet TMFs at
265 water depths between 1200 and 1800 m (Fig. 3 and Table 1). These features were also
266 identified by Rise et al. (2009). The ridges are almost perpendicular to the contours, indicating
267 that their overall form is a result of erosion by downslope oriented and gravity-driven
268 processes (Rise et al., 2009). Their present relief is also due to erosion from a number of
269 smaller slides (Fig. 5A). The ridges consist of stiff sediments (Bellec et al., 2012a; b).
270 Internally, the ridges are characterized by medium- to high-amplitude reflections, which are
271 truncated by the seabed (Fig. 7). Hence, the high-relief ridges are interpreted to be erosional
272 remnants in conformity with Rise et al. (2009). The ridges are deposits from seismic unit S2,
273 i.e. they are interpreted to represent an early glaciomarine to glaciofluvial phase of TMF
274 growth (Rydningen et al., submitted), and they thus protrude and pre-date the upper
275 succession of the TMFs (Fig. 4B).



276

277 **Fig. 7: Seismic profile across the erosional remnants (ER) and channels (C). Internal reflections within the**
 278 **erosional remnants are truncated by the seabed. See Fig. 3 for location.**

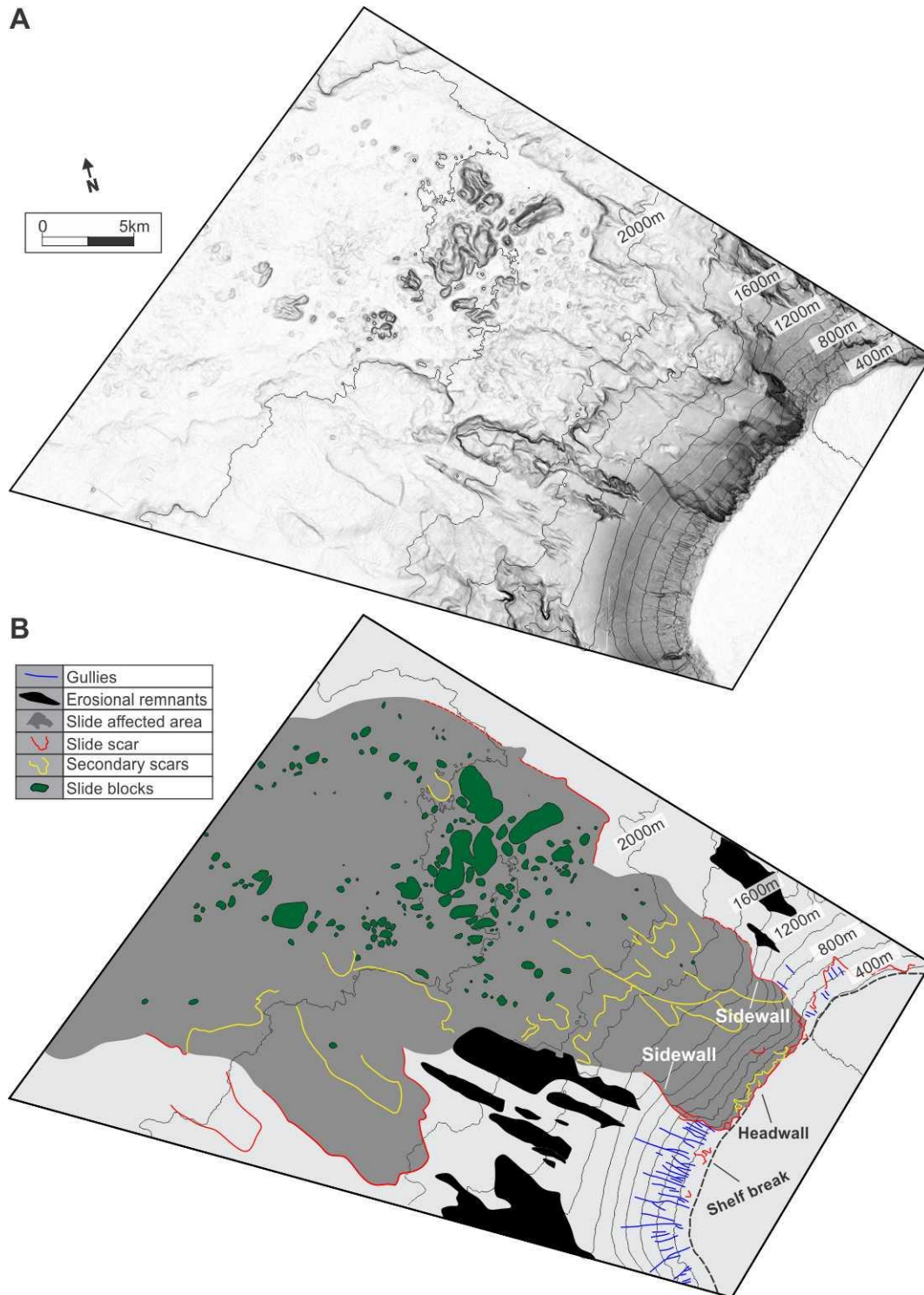
279 4.3.3 Large-scale sliding – the Andøya Slide

280 The Andøya Slide is located on the central part of the Andfjorden TMF (Fig. 8). The slide
 281 scar is characterized by a pronounced bathymetric depression on the upper slope and a distinct
 282 headwall up to 300 m high, which cuts into the outer shelf. The slide scar has steep sidewalls
 283 up to 200 m high. Smaller, amphitheatre-like shaped scars, typically between 250 and 500 m
 284 wide, occur within the upper slide scar, some places forming a stair-case pattern (Fig. 8).
 285 Below these, down to 1700 m water depth, the seabed within the slide has a relatively low
 286 relief. Secondary escarpments and small slide blocks characterize the seabed morphology
 287 downslope from ~1700 m water depth. The slide scar keeps its width (between 7 and 11 km)
 288 to a water depth of ~2100 m, i.e. where the slope gradient is below 2°. Further downslope, the
 289 Andøya Slide has affected parts of the Senja Canyon, and the slide widens to more than 20
 290 km. Large slide blocks dominate the morphology here (Fig. 8 and Table 1), and the displaced
 291 mass of remobilized sediments is characterized by a chaotic seismic facies (Fig. 9).

292 The relatively smooth seabed within the upper parts of the Andøya Slide, and the absence of
 293 high-relief ridges in this area, show a complete evacuation of failed masses. Within the slide
 294 scar, the stair-case pattern of scars indicates that sediments to different levels were affected.
 295 The sediment blocks are probably detached blocks of more consolidated sediments that
 296 moved for some distance and then stopped. These could originate from erosion of downslope-

297 oriented ridges described above, which do not occur within the slide scar. Further into the
298 basin (outside the data coverage), three large debris flow lobes have been identified
299 (Dowdeswell et al., 1996; Laberg et al., 2000), implying a total run-out distance of at least
300 190 km for this event.

301 The sliding on the Andfjorden TMF conforms to most large-scale mass-movements on the
302 Norwegian continental slope in that it cuts back all the way to the continental shelf break. The
303 failures stop at the flat lying and overconsolidated glacial deposits, as for example the
304 Storegga (Bugge et al., 1987; Haflidason et al., 2004), Trænadjupet (Laberg and Vorren,
305 2000) and Hinlopen-Yermak landslides (Vanneste et al., 2006). From the available seismic
306 data, it is difficult to verify the nature of the base slide scar, i.e. if it is parallel to underlying
307 strata and thus, if a stratigraphic interval within contouritic sediments represented a slip plane
308 for the failure – as has been found to characterize other slides on the Norwegian slope (e.g.
309 Bryn et al., 2005). This is due to low vertical resolution of the 2D seismic data and noise from
310 the gullied seabed.



311

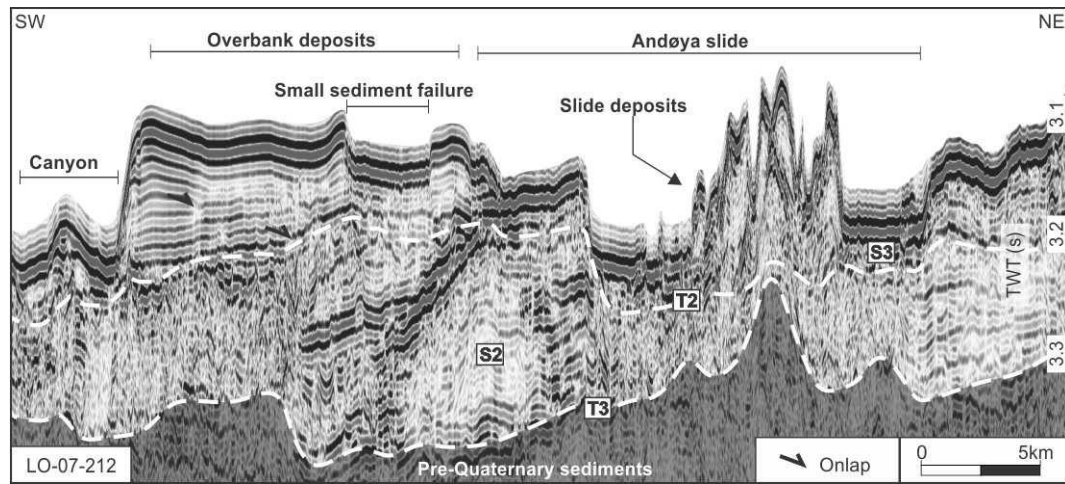
312 **Fig. 8: The Andøya Slide on the Andfjorden Trough Mouth Fan. See Fig. 3 for location. A: Slope gradient**

313 **map. B: Interpretation of A with the slide affected area in dark grey. The headwall of the Andøya Slide**

314 **cuts into the shelf. Smaller amphitheatre-like scars, in places forming a stair-case pattern, occur in the**

315 **uppermost part, while a low-relief terrain characterizes the slide scar down to 1700 m water depth.**

316 **Secondary escarpments and small slide blocks characterize the seabed morphology further downslope.**



317

318 **Fig. 9: Seismic profile crossing the Andøya Canyon, with its ancillary overbank deposits, and the Andøya**
 319 **Slide. Slide deposits within the Andøya Slide, which may constitute erosional remnant ridges, are**
 320 **indicated. See Fig. 3 for location.**

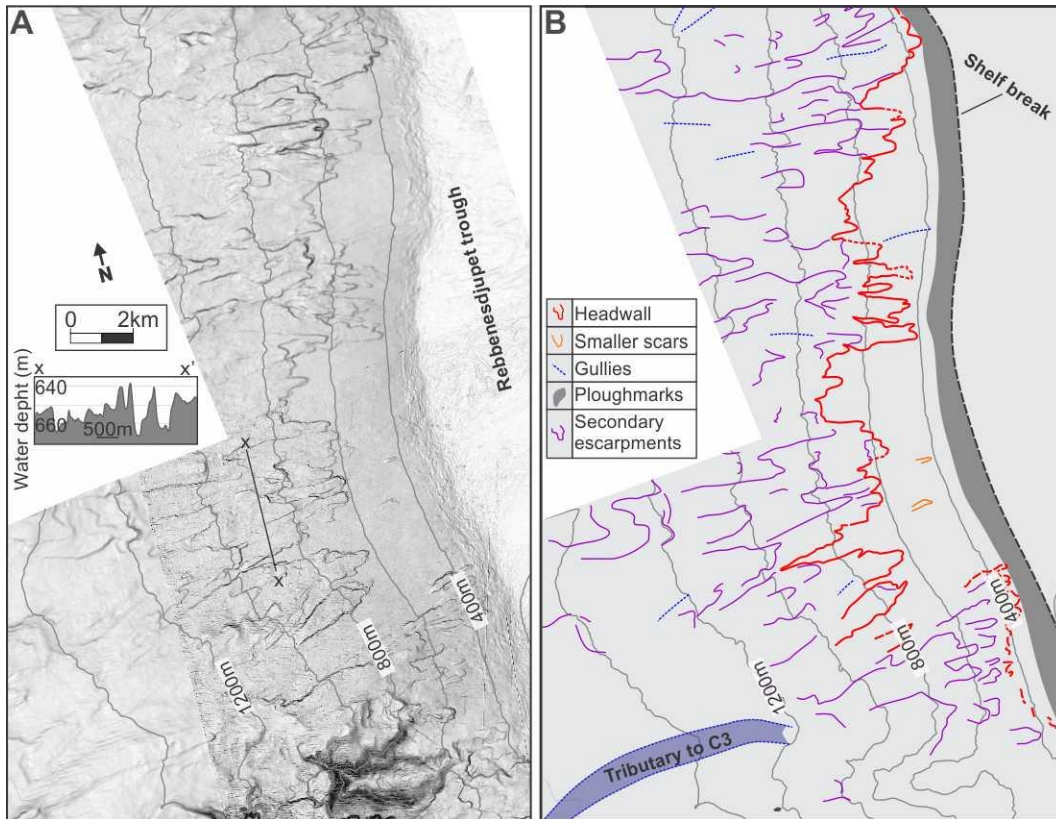
321 4.3.4 Smaller slides – the upper Rebbenesdjupet TMF

322 The upper part of the Rebbenesdjupet TMF is dominated by a number of smaller landslides.
 323 Sliding has occurred downslope from a water depth of 400 to 600 m, between 100 and 300 m
 324 below the shelf break, and downslope to ~1300 m (Fig. 3). The slide scars includes irregular
 325 headwalls and several secondary escarpments, forming a stair-case pattern of scars that are
 326 typically between 10 and 30 m high (Fig. 10).

327 The headwalls include several smaller, amphitheatre-shaped segments. No sediment ridges or
 328 blocks were observed within the scars, indicating complete evacuation of the failed masses.
 329 The area upslope of the headwall is nearly completely devoid of landforms; except for a few
 330 smaller individual slides and gullies, and iceberg ploughmarks immediately below the shelf
 331 break (Fig. 10). Downslope from ~1300 m water depth, the slide scars become more indistinct
 332 and a subdued channel between 10 and 20 m deep and 2 to 3 km wide is observed (Fig. 3).

333 The stair-case slide scar configuration on the upper Rebbenesdjupet TMF indicates a
 334 retrogressive landslide development, similar to the Style 2 mass-movement identified by
 335 Baeten et al. (2013) on the continental slope offshore the Lofoten Islands (south of our study

336 area). There, the headwall position was explained by an upslope decrease in slope gradient.
 337 The slope angle of the Rebbenesdjupet TMF, however, is gently increasing upslope making
 338 the influence of gradient less likely. Alternatively, this could be related to variations in
 339 composition and/or physical properties of the sediments of the upper Rebbenesdjupet TMF.
 340 Further studies are needed in order to clarify this.

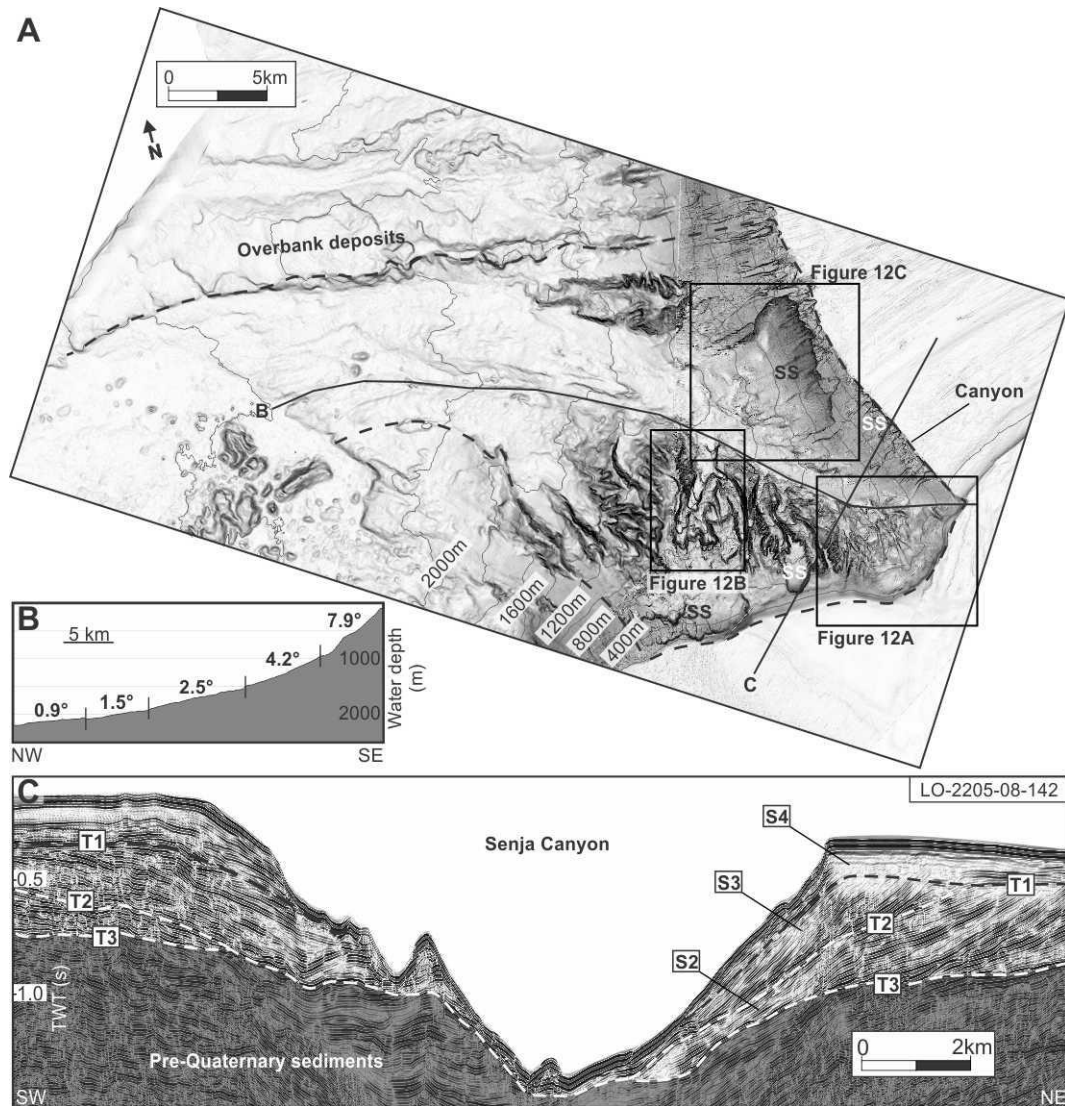


341
 342 **Fig. 10: The upper part of the Rebbenesdjupet Trough Mouth Fan. See Fig. 3 for location. A: Slope**
 343 **gradient map. Profile: The height of the slide scars is approximately between 10 and 30 m. B:**
 344 **Interpretation of A. A number of smaller landslides dominate the seabed morphology down to a water**
 345 **depth of ~1300 m. The slide headwall is irregular, and several secondary escarpments form a stair-case**
 346 **pattern downslope.**

347 **4.4 Inter-Trough Mouth Fan morphology**

348 4.4.1 The Senja Canyon

349 A submarine canyon, here named the Senja Canyon, is located between the Andfjorden and
350 Malangsdjupet TMFs. It is ~35 km long, as measured from the headwall to 2200 m water
351 depth, and represents a curved feature incised into the continental slope and outer shelf. The
352 headwall width is 6 km, and the canyon widens to a maximum of 20 km seaward (Fig. 11A).
353 A topographic long-profile from the headwall shows an overall concave shape with channel
354 gradient declining away from the shelf break (Fig. 11B). The canyon is V-formed in cross
355 section, and it cuts into a maximum of 1000 m of inferred Quaternary sediments (Fig. 11C)
356 (Rydningen et al., submitted).



357

358 **Fig. 11: The Senja Canyon. A: Slope gradient map of the Senja Canyon (outlined with dashed line).**

359 **Overbank deposits are indicated. Profiles in B and C, as well as Fig. 12, are indicated. See Fig. 3 for**

360 **location. B: Topographic long-profile from the headwall of the canyon. The Senja Canyon has an overall**

361 **concave shape with channel gradients declining downslope. C: Seismic profile across the inner part of the**

362 **canyon. The maximum incision of the canyon is 1000 m and it cuts into sediments of Quaternary age.**

363 The uppermost part of the headwall forms the present shelf break at between 100 and 200 m

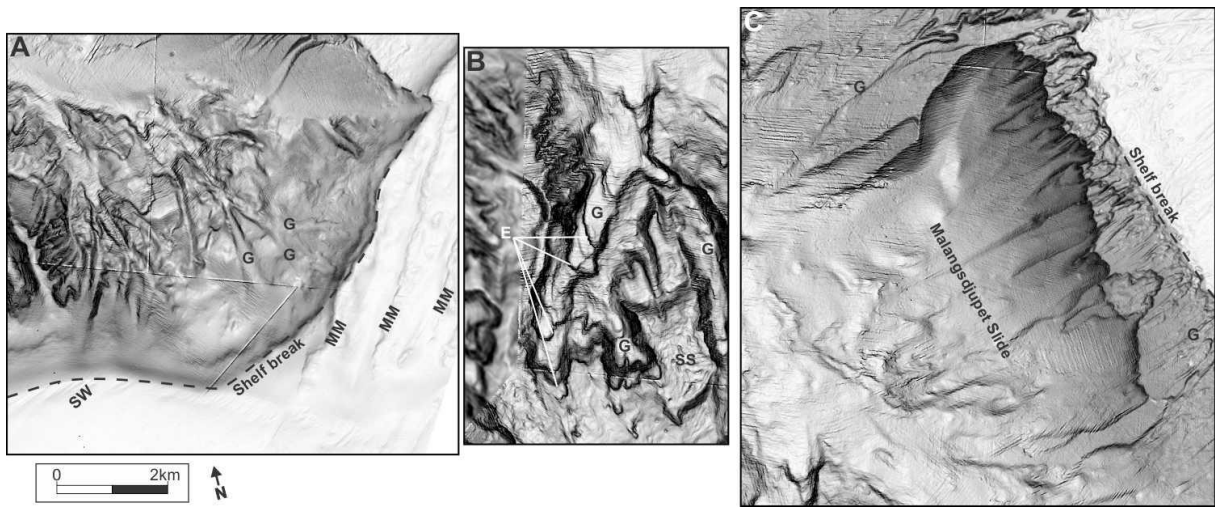
364 water depth. Marginal moraines are situated at and close to the shelf break (Rydningen et al.,

365 2013), and sediment ridges, indicating modern deposition of sandy sediments, tangentially

366 approach the western part of the headwall area (Fig. 12A). The headwall morphology is

367 smooth in its upper part and gullies originate a couple hundred meters below the shelf break.

368 These are partly buried in their upper reaches and coalesce with the main canyon channel
369 downslope (Fig. 12A).



370

371 **Fig. 12: Slope gradient maps of the Senja Canyon showing details of the headwall area (A), the western**
372 **sidewall (B), and the eastern sidewall (C). See Fig. 11 for location. A: Marginal moraines (MM) and**
373 **sediment waves (SW) are situated at and close to the shelf break. The canyon headwall is characterized by**
374 **partly buried gullies (G) which join downslope. B: Slide scars (SS) and steep-sided gullies dominate the**
375 **morphology on the western sidewall. Escarpments (E) are common along the gully thalwegs. C: Slide scars**
376 **and gullies also dominate the eastern sidewall. The largest slide, the Malangsdjupet Slide, extends down to**
377 **the base of the Senja Canyon.**

378 The western sidewall forms part of the northern slope of the Andfjorden TMF. Close to the
379 headwall, the western sidewall is smooth down to a water depth between 200 and 500 m,
380 except for a submarine landslide (Fig. 11A). West of this, another slide dominates down to
381 between 800 and 900 m (Fig. 11A). Further downslope, steep-sided gullies extend down to
382 the base of the canyon (Fig. 11A, 12B and Table 1). The gullies are sinuous, and consist of
383 several smaller tributary gullies. V-shaped escarpments are common along the gully thalwegs,
384 indicating areas of higher erosion (Fig. 12B).

385 The eastern sidewall forms part of the southern slope of the Malangsdjupet TMF, and is also
386 dominated by slides and gullies. The largest slide, here named the Malangsdjupet Slide, is

387 characterized by a distinct bathymetric depression and clear-cut sidewalls, which extends
388 down to the base of the Senja Canyon (Fig. 12C).

389 The main channel is the continuation of the gullies originating at the shelf break and can be
390 traced downslope to the Andøya Slide. The channel most likely coalesced with the Lofoten
391 Basin Channel outside the study area (Amundsen et al., 2015). Between 900 and 1600 m
392 water depth the channel is between 1 and 2 km wide and relatively flat. Beyond this, the
393 thalweg widens to ~10 km at 2200 m water depth. The inner, deeper part of the main channel
394 keeps its identity to a water depth of ~2000 m, where it branches out (Fig. 11A). In its lower
395 reaches, the northern part of the channel cuts into a weakly stratified sequence (Fig. 6). These
396 sediments are probably overbank deposits accumulated from turbidity currents transported
397 down the canyon channel, i.e. debris derived from the Andfjorden and Malangsdjupet TMFs.
398 Channel C1 and C2 also erode these deposits. Similar overbank sediments are observed north
399 of the Andøya Canyon channel (Fig. 9) (Laberg et al., 2005b; Amundsen et al., 2015).

400 In summary, the Senja Canyon owes its origin from an interplay of depositional and erosional
401 processes. Both sidewalls are part of the TMFs immediately to the north and south, and
402 sediment failure here, as well as in the headwall area generated gravity currents, focused into
403 the deeper area between the fans where they eroded and thus deepened and widened the
404 canyon. Glacigenic sediments from the Fennoscandian Ice Sheet at or near the shelf break,
405 and sandy sediments from ocean current winnowing during interglacial conditions, were
406 probably also routed through the canyon.

407 4.4.2 The continental slope west of the Malangsgrunnen bank

408 The shelf break at the outer Malangsgrunnen bank is concave. The continental slope has a
409 concave long-profile, and the slope gradient is in general steeper than 5° down to ~1500 m
410 water depth, before it decreases to below 2° at ~1800 m (Fig. 2B).

411 Slide scars which are sub-parallel to the shelf break dominate the upper slope morphology.
412 These occur approximately between 100 and 200 m below the shelf break, and are less fresh-
413 looking in the south (Fig. 5). Straight gullies occur downslope of the slide scars. These are
414 best developed in the south, where they are typically 500 m wide, 60 m deep and extend down
415 to 1100 m water depth. The gullies include one or two “waterfalls”, below which they are
416 wider (between 500 and 1200 m) and eroded to a deeper stratigraphic level. The gullies form
417 a dendritic pattern merging into one channel at ~1700 m water depth. This channel merges
418 with the C3 channel on the lowermost slope.

419 The slide scars are morphologically very similar to the slide scars on the upper
420 Rebbenesdjupet TMF. The straight gullies have a similar morphology as the gullies on the
421 upper TMFs, and are thus inferred to be of similar origin, i.e. formed by erosion from
422 sediment-laden bottom currents during LGM or by small-scale sediment failures. Downslope,
423 they merge with deeper gullies that were probably formed by retrogressive and small-scale
424 mass-wasting, originating at the lower parts of the slope. Due to the overall concave-shaped
425 form of the shelf break and its concave long-profile, the gully-forming flows originating at the
426 shelf break were routed into the deeper gullies. The overall form of the slope acted as a funnel
427 in focusing the downslope flow, forming the dendritic flow pattern.

428 To summarize, sediments originating from the northern Malangsdjupet TMF, as well as the
429 continental slope immediately to the north, have been routed through the depression between
430 the Malangsdjupet and Rebbenesdjupet TMFs. This did not, however, lead to the development
431 of a typical canyon morphology including a V-formed cross-section, as observed in the Senja
432 and Andøya canyons, possibly because less sediment was routed through this part of the
433 slope. This may be due to little input from the area of the Rebbenesdjupet TMF, where mainly
434 smaller slide scars have been identified.

435 **5 Discussion**

436 Below, the morphology and sedimentary processes of the studied high-gradient TMFs are
437 addressed, before the findings in this study are compared to the results from high-gradient
438 TMFs located elsewhere. Finally, sedimentary processes on high- and low-gradient TMFs are
439 compared.

440 **5.1 Morphology and sedimentary processes on high-gradient trough mouth fans on the**
441 **Troms margin**

442 The Malangsdjupet TMF is dominated by gully-channel complexes, and similar landforms are
443 also found on the Andfjorden TMF. Thus, the evolution of both fans included sediment
444 transport and distribution through gully-channel complexes. The Andfjorden TMF has more
445 recently been affected by a large submarine landslide, which remobilized much of these
446 complexes. The gradient and morphology of the Rebbenisdjupet TMF differs from the other
447 fans: the gradient is lower, the studied part of the upper fan is dominated by a number of small
448 and relatively shallow slide scars, and no upper-slope gullies have been identified. A similar
449 morphology has not previously been reported from other TMFs; the only area of comparable
450 features occurs on the continental slope offshore the Lofoten Islands (Fig. 1), an area
451 dominated by contouritic sediments and glaciomarine deposits (Laberg et al., 2005a; Baeten
452 et al., 2013). Thus, it is suggested that the uppermost succession on the Rebbenisdjupet TMF
453 is dominated by glaciomarine and/or contouritic sediments affected by repeated small-scale
454 sediment failure.

455 The difference between the upper succession of the Rebbenisdjupet TMF and the
456 Malangsdjupet/Andfjorden TMFs may be related to the oceanography of the area. The
457 Rebbenisdjupet TMF is located where the alongslope flowing Norwegian Atlantic Current
458 splits into two branches: one flows north along the Barents Sea slope, while the other flows
459 east entering into the Barents Sea. The two southern fans are located below the Norwegian

460 Atlantic Current (Hansen and Østerhus, 2000; Slubowska-Woldengen et al., 2008). It is
461 speculated here that this current is mainly erosive where it affects the upper Andfjorden and
462 Malangsdjupet TMFs, whereas deposition of contouritic sediments on the upper part of the
463 Rebbenesdjupet TMF is related to a reduction in flow speed and/or a reduction of the water
464 depth influenced by the Atlantic Current occurring where the modern current is splitting into
465 two branches. Further studies are needed in order to verify this.

466 No contouritic sediments are observed on the available data, except for the indirect evidence
467 by the small-scale sliding on the Rebbenesdjupet TMF. Thus, the main sediment input onto
468 the TMFs has most likely occurred during peak glacials when fast-flowing ice streams within
469 the Fennoscandian Ice Sheet transported sediments in an active subglacial layer to the
470 grounding-line at the shelf break (Vorren and Plassen, 2002; Ottesen et al., 2005; Rydningen
471 et al., 2013). The overall convex fan form and progradational seismic facies (Fig. 4;
472 Rydningen et al., submitted) show that this muddy diamicton (Vorren et al., 1984) was
473 repeatedly distributed onto the fan. On the Andfjorden and Malangsdjupet TMFs, gully-
474 channel complexes occur within such deposits. It is inferred that the steep slope of these high-
475 gradient TMFs promoted rapid transformation from small-scale slumps and debris flows on
476 the upper slope, into partly erosive turbidity currents. This is because turbidity currents are
477 known to have led to the formation of channel systems elsewhere in both high-latitude (e.g.
478 Dowdeswell et al., 2004) and low-latitude (Posamentier and Kolla, 2003) continental margins.
479 Also, similar gully-channel systems have not, in most cases, been reported from low-gradient
480 TMFs dominated by GDF deposits (e.g. Laberg and Vorren, 1995; King et al., 1996; Davison
481 and Stoker, 2002; García et al., 2012). The transformation from debris flows into turbidity
482 currents, which involves extensive dilution of debris-flow material, observed in experiments
483 by Hampton (1972), is probably a consequence of flow transformation due to the relatively
484 high velocity caused by the steep slope gradient (Fisher, 1983). The transition from gullies to

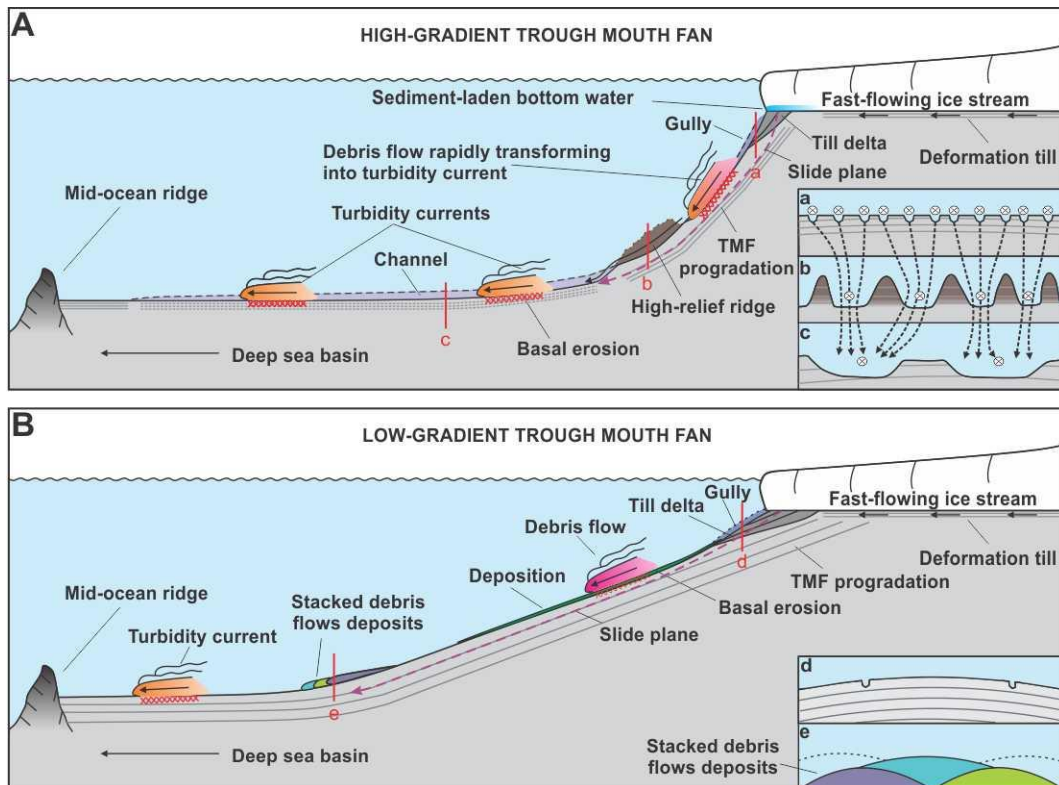
485 channels was probably controlled by the relief of the slope and the high-relief ridges, which
486 routed the turbidity currents downslope.

487 Part of the turbidity currents originating from the upper Andfjorden and Malangsdjupet TMFs
488 were routed into the Andøya and Senja Canyons, as well as the channel complex between the
489 Malangsdjupet and Rebbenedjupet TMFs, showing that the inter-TMF areas have also, to a
490 large degree, evolved as a response to sediment input to the fans. These currents were erosive,
491 forming the canyon thalwegs, and probably also influenced on the stability of the TMF
492 deposits, triggering smaller and larger landslides by undercutting. As the channel at the mouth
493 of the Senja Canyon turns south-westward in the lower part of the Andøya Slide, it is
494 suggested that undercutting may also have influenced the stability of the continental slope
495 sediments in the central part of the Andfjorden TMF.

496 The Andøya Slide affected part of the Andfjorden TMF and smaller slide scars are frequent
497 on the continental slope off Troms. TMFs represent sediment depocentres that may be
498 unstable due to periods of high sedimentation rate, and submarine landslides of size
499 comparable to the Andøya Slide or larger have repeatedly affected other TMFs along the
500 Norwegian – Barents Sea – Svalbard margin (Laberg and Vorren., 1993; 2000; Bryn et al.,
501 2005; Vanneste et al., 2006). The Andøya Slide has been suggested to be of late glacial –
502 Holocene age (Laberg et al., 2000). The results from this study support this interpretation, as
503 progradation of glacial sediments, and gullies, mainly inferred to be of glacial origin, have
504 not been identified within the slide scar.

505 From the above results a conceptual model has been compiled, summarizing the sedimentary
506 processes acting on high-gradient TMFs (Fig. 13A). The model is based on the results from
507 the fans of highest gradient, i.e. the Andfjorden and Malangsdjupet TMFs. In the model, large
508 volumes of subglacial debris were transported beneath fast-flowing ice streams to the shelf

509 break. These sediments were deposited as progradational units, which were subsequently
 510 partly subjected to a downslope remobilization as erosive turbidity currents forming gullies.
 511 Furthermore, high-relief ridges routed the turbidity currents into channels which may have
 512 continued into the deep sea basin. Also included in the model is large-scale sliding which may
 513 modify the morphology of high-gradient TMFs (Fig. 13A).



514
 515 **Fig. 13: Conceptual models of high-gradient (A) and low-gradient (B) trough mouth fans. See text for**
 516 **further discussion.**

517 **5.2 High-gradient trough mouth fans in other areas**

518 Seaward-bulging depocentres with high gradients are found at glacial trough mouths at both
 519 northern and southern high latitudes (Table 2), and they are here regarded as high-gradient
 520 TMF-equivalents. In total, ten high-gradient TMFs (slope gradient $>4^\circ$) have been identified
 521 outside high Arctic cross-shelf troughs (not including the Troms margin), including areas off
 522 South and East Greenland, Queen Elisabeth Island, and in the Baffin Bay (Batchelor and

523 Dowdeswell, 2014). Also, high-gradient TMFs are found on the margin off the Antarctic
524 Peninsula (Table 2) (Tomlinson et al., 1992; Larter and Cunningham, 1993; Dowdeswell et
525 al., 2004; Amblas et al., 2006).

526 Previous studies on high-gradient TMFs generally suffer from a limited access of bathymetric
527 data (Table 2). An exception is the study by Amblas et al. (2006) off the Antarctic Peninsula,
528 where swath-bathymetric data covering the inner shelf to the lower slope has been acquired.
529 There, gullies at the upper slope and canyon-channel systems on the continental rise together
530 form a complex dendritic pattern. However, the gullies vanish at the base of the slope,
531 showing no apparent connection with the canyon-channel system downslope. Large sediment
532 mounds are found between 500 and 1000 m above the canyon-channel axes, and are inferred
533 to have formed from settling of suspension clouds from turbidity currents, caused by the
534 considerable hydraulic jump at the base of the North Pacific Peninsula continental slope,
535 where the slope gradient shifts from more than 18° to less than 4° . On the high-gradient TMFs
536 on the continental margin off Troms, a mid-fan relief is instead dominated by high-relief
537 ridges which probably focused turbidity currents into the channels on the lower part of the
538 slope. Thus, the system described by Amblas et al. (2006) resembles the gully-channel
539 complex on the high-gradient TMFs in this study. Nevertheless, differences are found in the
540 transition from gullies to channels on the lower part of the slope. This may relate to the
541 presence or absence of high-relief ridges.

542 Based on seismic data, Clausen (1998) described modern scars in the uppermost part of high-
543 gradient TMFs on the SE Greenland margin and related these to slumps and slides. Canyons
544 are absent and gullies are scarce on this part of the margin, suggesting that ‘unchannelized
545 debris flows probably was the main process by which the slope prograded’ (Clausen, 1998).
546 Till deltas, deposited at the shelf edge from grounded ice, were subsequently subjected to
547 downslope redeposition, initiated as small-scale slope-failures. The sediment remobilization

548 generated GDFs on the slope, which was either deposited as GDF debrites at the lower slope
549 or passed into turbidity currents, identified from channels on the continental rise. As opposed
550 to the upper-slope gullies routing turbidity currents downslope on the continental slope off
551 Troms, the sediment transport across the upper TMFs on the SE Greenland margin appear to
552 have occurred through unchannelized flows. In this regard it should be mentioned that the
553 lack of gullies may reflect the data base available from this area, since gullies are most easily
554 identified on swath-bathymetric data. Further downslope, similar characteristics as the
555 Andfjorden and Malangsdjupet TMFs are found, with channels formed by turbidity currents
556 continuing into the deep sea basin. However, Clausen (1998) identified GDF debrites on the
557 lower slope, which are absent from the Troms margin TMFs.

558 In other studies on high-gradient TMFs off East Greenland (García et al., 2012) and the
559 Antarctic Peninsula (Tomlinson et al., 1992; Larter and Cunningham, 1992; Dowdeswell et
560 al., 2004) gullies on the upper slope merging into channels are common, testifying to turbidity
561 currents being the main mode of transport for sediments across the slope (Table 2). Broadly,
562 therefore, it is found that other high-gradient TMFs conform to the conceptual model shown
563 in Fig. 13A. GDF debrites are scarce or absent on high-gradient TMFs, similar to the TMFs
564 on the Troms margin. Also, gully-branching systems with similarities to the gully-channel
565 complexes found here have been described on the Antarctic margin (Tomlinson et al., 1992;
566 Dowdeswell et al., 2004; Amblas et al., 2006), and possibly on the East Greenland margin
567 (García et al., 2012). In these areas, however, turbidity currents are inferred to form sediment
568 waves or sediment mounds on the lower slope, probably as a consequence of the lower slope
569 velocities caused by a gradient decrease. In contrast, turbidity currents are channelized
570 through high-relief ridges on the Troms margin TMFs, thus maintaining their velocity
571 downslope, and forming channels on the lower slope. Finally, downslope sediment transport

572 from small-scale slides is common in other high-gradient TMFs, while large-scale slides are,
573 unlike in this study, not described.

574 **5.3 Processes on high- and low-gradient trough mouth fans – a comparison**

575 Processes on the low-gradient end member of TMFs are well-studied (e.g. Vorren et al., 1989;
576 Aksu and Hiscott, 1992; Vogt et al., 1993; Laberg and Vorren, 1995; King et al., 1996, 1998;
577 Dowdeswell et al., 2008) (Fig. 13B). GDFs, originating at the upper slope, are found to extend
578 onto the abyssal plain (Fig. 13B). The individual GDF debrites, the “building blocks” of low-
579 gradient TMFs, can be mapped by side-scan sonar (Vogt et al., 1993) and swath-bathymetric
580 data (Davison and Stoker, 2002), while buried debrites can be identified from seismic data as
581 stacked mound forms extending downslope, deposited between older debrites (Laberg and
582 Vorren, 1995; 1996a; b; King et al., 1996; Vorren and Laberg, 1997). The debris flows
583 terminate on the lower fan, probably due to a decrease in slope gradient, and may continue as
584 turbidity currents further into the basin (Fig. 13B). Work from the Bear Island TMF show that
585 the lithologies of GDF debrites on the slope are similar to the till on the shelf, i.e. that little or
586 no sediment sorting has taken place during downslope flow (Laberg and Vorren, 1995).

587 The TMF gradients are inferred to exert a fundamental control on the sedimentary processes
588 and, hence, on the resulting TMF morphology and sediment composition (Ó Cofaigh et al.,
589 2003; Piper and Normark, 2009). The gentler slope of low-gradient TMFs facilitate
590 incremental outbuilding of the fan by debris-flow deposition, and would prevent rapid
591 reworking of debris into turbidity currents (Fig. 13B) (Ó Cofaigh et al., 2003). In contrast,
592 subglacial debris deposited at the Troms margin shelf break during peak glaciations was prone
593 to be reworked into turbidity currents due to higher flow velocity on the steep slope,
594 facilitating sediment transport into the deep sea (Fig. 13A), and thus maintaining the high
595 gradient of the slope (a positive feedback loop). Also, the input of glacial sediments to this
596 sector of the Norwegian margin was low compared to the areas to the north (Bear Island

597 TMF) and south (prograding wedge off Mid-Norway) (Rydningen et al., submitted), further
598 promoting a steep continental slope. The steep Troms margin slope was possibly inherited
599 from a likely original steep continental slope (Osmundsen and Redfield, 2011; Redfield and
600 Osmundsen, 2013; Indrevær et al., 2013), inferred to have exerted a fundamental control on
601 continental margin development throughout the late Pliocene – Pleistocene period of large-
602 scale glaciations reaching the shelf break as discussed by Rydningen et al. (submitted).

603 Gullies, merging downslope, occur on the upper parts of the low-gradient Bear Island and
604 Storfjorden TMFs in the SW Barents Sea (Laberg and Vorren, 1995; 1996a; Vorren et al.,
605 1998). These gullies have a fresh relief and do not appear to contain any sediment infill,
606 indicating that they were not formed during full-glacial conditions (Vorren et al., 1998). No
607 gully-channel complexes were described on these fans. The low-angle Belgica TMF on the
608 Antarctic margin has, on the other hand, a well-developed network of gullies and channels,
609 interpreted to be related to the intermittent downslope transfer of sediments from the upper
610 slope to the continental rise through turbidity currents (Dowdeswell et al., 2008). Some of
611 these gullies are observed to cut through debrites on the slope, and the inferred turbidity-
612 derived debris is overlying these. Thus, the processes taking place during the formation of the
613 gullies were probably active during late stages of the peak glaciation and the following
614 deglaciation, and possibly in phases subsequent to this.

615 In general, it appears that gullies on low-gradient TMFs post-date GDF activity and thus,
616 mainly formed during the end of the LGM, the deglaciation, or subsequent to this (Vorren et
617 al., 1998; Dowdeswell et al., 2008). In this study, it is observed both fresh-looking gullies,
618 which probably originated as sediment-failures, and less fresh-looking gullies, inferred to
619 have formed during full-glacial conditions by either sediment-laden bottom waters or small-
620 scale failures. In any case, the gullies are inferred to have formed from turbidity currents
621 originating at the steep upper slope (Fig. 13A). In contrast, on the low-gradient TMFs, debris

622 flows formed on the upper slope. These eroded the substrate to a lesser degree, and deposited
623 sediments as they moved downslope (Fig. 13B).

624 Large submarine slide scars on TMFs are well-studied from the Norwegian margin, including
625 slide scars on the Bear Island TMF (Laberg and Vorren, 1993), the Hinlopen-Yermak TMF
626 (Vanneste et al., 2006) and the North Sea TMF (Bryn et al., 2005). On other glaciated
627 margins, such as the East Greenland margin (Vorren et al., 1998) and on the Belgica TMF
628 (Dowdeswell et al., 2008), no major slide scars have been revealed on the seabed. On the
629 Troms margin, the Andøya Slide has remobilized major parts of the Andfjorden TMF, while
630 only smaller-scale mass-movements have occurred on the other TMFs, with the exception of
631 the Malangsdjupet Slide. Thus, large-scale sliding can occur at both high-and low-gradient
632 TMFs.

633 In summary, it is found that high-gradient TMFs facilitate the evolution of erosive turbidity
634 currents, which contrasts with the low-gradient end member of TMFs where GDFs dominate.
635 Also, the high number of gullies on the steep part of the Troms margin TMFs, with ancillary
636 channels downslope, were likely important pathways for sediments across the slope,
637 maintaining the steepness of the TMFs (Fig. 13A). Gullies on low-gradient TMFs are
638 generally formed in late glacial and deglacial phases, and are thus not important for
639 downslope flow during full-glacial conditions. Catastrophic events in the form of large-scale
640 submarine landslides occur at both end members of TMFs.

641

642 **6 Conclusions**

- 643 • On the continental slope off Troms, northern Norway, the complex morphology of three
644 high-gradient trough mouth fans (TMF) situated seaward of formerly glaciated cross-shelf
645 troughs, as well as inter-fan areas, show extensive evidence of downslope transfer of
646 sediments, involving formation of gullies, channels and slides.
- 647 • The Malangsdjupet TMF is dominated by gully-channel complexes, which is also found
648 on the Andfjorden TMF outside an area dominated by a large submarine landslide (the
649 Andøya Slide). Thus, both fans evolved by sediment transport and distribution through
650 gully-channel complexes, while the Andfjorden TMF was affected by a large submarine
651 landslide which remobilized much of these complexes.
- 652 • The Rebbenesdjupet TMF has a lower gradient and is dominated by a number of small
653 and relatively shallow slide scars, inferred to be related to small-scale sediment failure of
654 glaciomarine and/or contouritic sediments.
- 655 • The Andøya and Senja canyons, as well as the Malangsgrunnen inter-fan slope, make up
656 the inter-fan areas. The canyons were cut into the adjacent TMFs, and they deepened and
657 widened as turbidity currents were routed downslope. Mass-movements within the study
658 area seem to have been triggered by undercutting from the canyons. The overall form of
659 the Malangsgrunnen shelf break and inter-fan slope acted as a funnel in focusing
660 downslope flow from upper-slope gullies and slides.
- 661 • The sedimentary processes on the high-gradient TMFs off Troms are summarized in a
662 conceptual model. The main sediment input occurred during peak glacials when the
663 Fennoscandian Ice Sheet reached the shelf edge and distributed glacial sediments onto
664 the fans. Gully-channel complexes occur within these deposits on the Andfjorden and
665 Malangsdjupet TMFs, which indicates that the steep slope of these fans promoted rapid
666 transformation from small-scale slumps and debris flows on the upper slope, into partly

667 erosive turbidity currents. These may have extended into the deep sea, thus promoting
668 efficient sediment by-pass across the TMFs. This model can be applied to other high-
669 gradient TMFs situated at the mouths of other glaciated cross-shelf troughs.

- 670 • The TMF slope gradients are inferred to exert a fundamental control on the sedimentary
671 processes and, hence, on the resulting TMF morphology and sediment composition. The
672 building blocks for low-gradient TMFs, glaciogenic debris flow debrites, are missing on the
673 studied high-gradient TMFs. Instead, gully-channels complexes dominate, which are rare
674 on low-gradient TMFs. Large-scale sliding appears to occur on both high- and low-
675 gradient TMFs.

676

677 **7 Acknowledgements**

678 This work was financially supported by the Research Council of Norway and DONG E&P
679 Norge AS through their funding of an Industrial Ph.D. position to the first author. We are
680 grateful to the Norwegian Petroleum Directorate for permission to publish the seismic data
681 shown in Fig. 9 and 11C. We thank Bedford Institute of Oceanography for hosting the first
682 author during his research stay in Halifax the fall of 2012. Special thanks to Edward (Ned)
683 King, David Mosher, David Piper, Hans Petter Sejrup and Martyn Stoker for valuable
684 discussions. Mariana da Silveira Ramos Esteves kindly commented on the English text.
685 Finally, we thank Editor Takashi Oguchi and referees Pedro P. Cunha and Bernhard Bauer for
686 their constructive reviews. Professor Tore O. Vorren (deceased 16.06.13) was the main
687 supervisor for T.A. Rydningen during his Ph.D. studies. Professor Vorren passed away in
688 June 2013 and we dedicate this paper to his memory.

689 **8 Figure captions**

690 Fig. 1: Bathymetric map of the Norwegian Sea and the SW Barents Sea generated from the
691 IBCAO database (Jakobsson et al., 2012). Contour interval is 200 m. The study area is
692 indicated by the white box.

693 Fig. 2: The area of study. A: Bathymetric map of the continental shelf and slope outside
694 Troms County, northern Norway. The dashed lines delimit data sets with different spatial
695 resolution. B: Dip map of the seabed.

696 Fig. 3: The outer continental shelf and upper slope off northern Norway. See Fig. 2 for
697 location. A: Slope gradient map.. Areas of steep slopes have a darker colour. Locations of
698 detail figures and seismic lines are indicated. B: Interpretation of landforms discussed in this
699 paper. TMF=Trough Mouth Fan.

700 Fig. 4: Seismo-stratigraphic framework of the late Cenozoic sediments on the Troms margin
701 (adopted from Rydningen et al., submitted). See Fig. 3 for location of profiles. A: Composite
702 seismic strike line crossing the study area. B: Seismic dip line crossing the shelf break in the
703 Malangsdjupet trough.

704 Fig. 5: The Malangsdjupet Trough Mouth Fan and the Malangsgrunnen inter-fan slope. See
705 Fig. 3 for location. A: Slope gradient map. Red arrows indicate slide scars on erosional
706 remnants. B: Interpretation of A. Gullies dominate the Trough Mouth Fan morphology down
707 to 1200 m water depth, before they merge into channels on the lower slope (C1, C2 and C3).
708 The depths of the channels are illustrated by a bathymetric profile. The Malangsgrunnen inter-
709 fan slope is dominated by slides and gullies forming a dendritic pattern merging into C3 on
710 the lower slope.

711 Fig. 6: Seismic profile across overbank deposits showing a weak internal stratification.
712 Channel C1 erodes into the overbank deposit and has a cut-and-fill character. A possible
713 palaeo-channel is located in the northern part of the Senja Canyon channel. See Fig. 3 for
714 location.

715 Fig. 7: Seismic profile across the erosional remnants (ER) and channels (C). Internal
716 reflections within the erosional remnants are truncated by the seabed. See Fig. 3 for location.

717 Fig. 8: The Andøya Slide on the Andfjorden Trough Mouth Fan. See Fig. 3 for location. A:
718 Slope gradient map. B: Interpretation of A with the slide affected area in dark grey. The
719 headwall of the Andøya Slide cuts into the shelf. Smaller amphitheatre-like scars, in places
720 forming a stair-case pattern, occur in the uppermost part, while a low-relief terrain
721 characterizes the slide scar down to 1700 m water depth. Secondary escarpments and small
722 slide blocks characterize the seabed morphology further downslope.

723 Fig. 9: Seismic profile crossing the Andøya Canyon, with its ancillary overbank deposits, and
724 the Andøya Slide. Slide deposits within the Andøya Slide, which may constitute erosional
725 remnant ridges, are indicated. See Fig. 3 for location.

726 Fig. 10: The upper part of the Rebbenesdjupet Trough Mouth Fan. See Fig. 3 for location. A:
727 Slope gradient map. Profile: The height of the slide scars is approximately between 10 and 30
728 m. B: Interpretation of A. A number of smaller landslides dominate the seabed morphology
729 down to a water depth of ~1300 m. The slide headwall is irregular, and several secondary
730 escarpments form a stair-case pattern downslope.

731 Fig. 11: The Senja Canyon. A: Slope gradient map of the Senja Canyon (outlined with dashed
732 line). Overbank deposits are indicated. Profiles in B and C, as well as Fig. 12, are indicated.
733 See Fig. 3 for location. B: Topographic long-profile from the headwall of the canyon. The
734 Senja Canyon has an overall concave shape with channel gradients declining downslope. C:
735 Seismic profile across the inner part of the canyon. The maximum incision of the canyon is
736 1000 m and it cuts into sediments of Quaternary age.

737 Fig. 12: Slope gradient maps of the Senja Canyon showing details of the headwall area (A),
738 the western sidewall (B), and the eastern sidewall (C). See Fig. 11 for location. A: Marginal
739 moraines (MM) and sediment waves (SW) are situated at and close to the shelf break. The
740 canyon headwall is characterized by partly buried gullies (G) which join downslope. B: Slide
741 scars (SS) and steep-sided gullies dominate the morphology on the western sidewall.
742 Escarpments (E) are common along the gully thalwegs. C: Slide scars and gullies also
743 dominate the eastern sidewall. The largest slide, the Malangsdjupet Slide, extends down to the
744 base of the Senja Canyon.

745 Fig. 13: Conceptual models of high-gradient (A) and low-gradient (B) trough mouth fans. See
746 text for further discussion.

747 **9 References**

- 748 Aksu, A.E., Hiscott, R.N., 1992. Shingled Quaternary debris flow lenses on the north-east
749 Newfoundland Slope. *Sedimentology* 39, 193-206.
- 750 Amblas, D., Urgeles, R., Canals, M., Calafat, A.M., Rebesco, M., Camerlenghi, A., Estrada,
751 F., De Batist, M., Hughes-Clarke, J.E., 2006. Relationship between continental rise
752 development and palaeo-ice sheet dynamics, Northern Antarctic Peninsula Pacific margin.
753 *Quaternary Science Reviews* 25, 933-944.
- 754 Amundsen, H.B., Laberg, J.S., Vorren, T.O., Haflidason, H., Forwick, M., Buhl-Mortensen,
755 P., 2015. Late Weichselian – Holocene evolution of the high-latitude Andøya submarine
756 Canyon, North-Norwegian continental margin. *Marine Geology* 363, 1-14.
- 757 Baeten, N.J., Laberg, J.S., Forwick, M., Vorren, T.O., Vanneste, M., Forsberg, C.F., Kvalstad,
758 T.J., Ivanov, M., 2013. Morphology and origin of smaller-scale mass movements on the
759 continental slope off northern Norway. *Geomorphology* 187, 122-134.
- 760 Batchelor, C.L., Dowdeswell, J.A., 2014. The physiography of High Arctic cross-shelf
761 troughs. *Quaternary Science Reviews* 92, 68-96.
- 762 Bellec, V.K., Bøe, R., Thorsnes, T., Rise, L., Dolan, M.F.J., Elvenes, S., Lepland, A., Hansen,
763 O.H., 2012a. Geologisk havbunnskart, Kart 69301600, September 2012, M 1: 100 000,
764 Norges Geologiske Undersøkelse.
- 765 Bellec, V.K., Bøe, R., Thorsnes, T., Rise, L., Dolan, M.F.J., Elvenes, S., Lepland, A., Hansen,
766 O.H., 2012b. Geologisk havbunnskart, Kart 70001600, September 2012, M 1: 100 000,
767 Norges Geologiske Undersøkelse.

768 Bellec, V.K., Dolan, M.F.J., Bøe, R., Thorsnes, T., Rise, L., Buhl-Mortensen, L., Buhl-
769 Mortensen, P., 2009. Sediment distribution and seabed processes in the Troms II area –
770 offshore North Norway. *Norwegian Journal of Geology* 89, 29-40.

771 Bryn, P., Berg, K., Forsberg, C.F., Solheim, A., Kvalstad, T.J., 2005. Explaining the Storegga
772 Slide. *Marine and Petroleum Geology* 22, 11-19.

773 Bugge, T., 1983. Submarine slides on the Norwegian continental margin, with special
774 emphasis on the Storegga area. The Continental Shelf and Petroleum Research Institute,
775 Trondheim, Publication 110, 152pp.

776 Bugge, T., Befring, S., Belderson, R.H., Eidvin, T., Jansen, E., Kenyon, N.H., Holtedahl, H.,
777 Sejrup, H.P., 1987. A giant three-stage submarine slide off Norway. *Geo-Marine Letters* 7,
778 191-198.

779 Buhl-Mortensen, L., Bøe, R., Dolan, M.F.J., Buhl-Mortensen, P., Thorsnes, T., Elvenes, S.,
780 Hodnesdal, H., 2012. Banks, troughs, and canyons on the continental margin off Lofoten,
781 Vesterålen, and Troms, Norway. In: Harris, P.T., Baker, E.K. (Eds.), *Seafloor geomorphology*
782 *as Benthic Habitat*. Elsevier Inc., Amsterdam, pp. 703-715, [http://dx.doi.org/10.1016/B978-0-](http://dx.doi.org/10.1016/B978-0-783)
783 [12-385140-6.00051-7](http://dx.doi.org/10.1016/B978-0-12-385140-6.00051-7).

784 Clausen, L., 1998. The Southeast Greenland glaciated margin: 3D stratal architecture of shelf
785 and deep sea. In: Stoker, M., Evans, D., Cramps, A. (Eds.), *Geological Processes on*
786 *Continental margins: Sedimentation, Mass-Wasting and Stability*. Geological Society,
787 London, Special Publications 129, pp. 173-203.

788 Dahlgren, K.I.T., Vorren, T.O., Stoker, M.S., Nielsen, T., Nygård, A., Sejrup, H.P., 2005.
789 Late Cenozoic prograding wedges on the NW European continental margin: their formation
790 and relationship to tectonics and climate. *Marine and Petroleum Geology* 22, 1089-1110.

791 Davison, S., Stoker, M.S., 2002. Late Pleistocene glacially-influenced deep-marine
792 sedimentation off NW Britain: implications for the rock record. In: Dowdeswell, J.A., Ó
793 Cofaigh, C. (Eds.), *Glacier-Influenced Sedimentation in High-Latitude Continental Margins*.
794 Geological Society, London, Special Publications 203, 129-147.

795 Dowdeswell, J.A., Kenyon, N.H., Elverhøi, A., Laberg, J.S., Hollender, F.-J., Mienert, J.,
796 Siegert, M.J., 1996. Large-scale sedimentation on the glacier-influenced polar North Atlantic
797 margins: Long-range side-scan sonar evidence. *Geophysical Research Letters* 23, 3535-3538.

798 Dowdeswell, J.A., Ó Cofaigh, C., Noormets, R., Larter, R.D., Hillenbrand, C.-D., Benetti, S.,
799 Evans, J., Pudsey, C.J., 2008. A major trough-mouth fan on the continental margin of the
800 Bellingshausen Sea, West Antarctica: The Belgica Fan. *Marine Geology* 252, 129-140.

801 Dowdeswell, J.A., Ó Cofaigh, C., Pudsey, C.J., 2004. Continental slope morphology and
802 sedimentary processes at the mouth of an Antarctic palaeo-ice stream. *Marine Geology* 204,
803 203-214.

804 Fisher, R.V., 1983. Flow transformations in sediment gravity flows. *Geology* 11, 273-274.

805 Gales, J.A., Forwick, M., Laberg, J.S., Vorren, T.O., Larter, R.D., Graham, A.G.C., Baeten,
806 N.J., Amundsen, H.B., 2013. Arctic and Antarctic submarine gullies – a comparison of high
807 latitude continental margins. *Geomorphology* 201, 449-461.

808 García, M., Dowdeswell, J.A., Ercilla, G., Jakobsson, M., 2012. Recent glacially influenced
809 sedimentary processes on the East Greenland continental slope and deep Greenland Basin.
810 *Quaternary Science Reviews* 49, 64-81.

811 Haflidason, H., Sejrup, H.P., Nygård, A., Mienert, J., Bryn, P., Lien, R., Forsberg, C.F., Berg,
812 K., Masson, D., 2004. The Storegga Slide: architecture, geometry and slide development.
813 *Marine Geology* 213, 201-234.

- 814 Hampton, M.A., 1972. The role of subaqueous debris flow in generating turbidity currents.
815 *Journal of Sedimentary Research* 42, 775-793.
- 816 Hansen, B., Østerhus, S., 2000. North Atlantic-Nordic Seas exchanges. *Progress in*
817 *Oceanography* 45, 109–208.
- 818 Hjelstuen, B.O., Eldholm, O., Faleide, J.I., 2007. Recurrent Pleistocene mega-failures on the
819 SW Barents Sea margin. *Earth and Planetary Science Letters* 258, 605-618.
- 820 Indrevær, K., Bergh, S. G., Koehl, J.-B., Hansen, J.-A., Schermer, E. R., Ingebrigtsen, A.,
821 2013. Post-Caledonian brittle fault zones on the hyperextended SW Barents Sea margin: New
822 insights into onshore and offshore margin architecture: *Norwegian Journal of Geology/Norsk*
823 *Geologisk Forening* 93, 167-188.
- 824 Jakobsson, M., Mayer, L.A., Coakley, B., Dowdeswell, J.A., Forbes, S., Fridman, B.,
825 Hodnesdal, H., Noormets, R., Pedersen, R., Rebesco, M., Schenke, H.-W., Zarayskaya, Y.A.,
826 Accettella, D., Armstrong, A., Anderson, R.M., Bienhoff, P., Camerlenghi, A., Church, I.,
827 Edwards, M., Gardner, J.V., Hall, J.K., Hell, B., Hestvik, O.B., Kristoffersen, Y., Marcussen,
828 C., Mohammad, R., Mosher, D., Nghiem, S.V., Pedrosa, M.T., Travaglini, P.G., Weatherall,
829 P., 2012. The International Bathymetric Chart of the Arctic Ocean (IBCAO) Version 3.0.
830 *Geophysical Research Letters* 39, <http://dx.doi.org/10.1029/2012GL052219>.
- 831 Kenyon, N.H., 1987. Mass-wasting features on the continental slope of Northwest Europe.
832 *Marine Geology* 74, 57-77.
- 833 King, E.L., Haflidason, H., Sejrup, H.P., Løvlie, R., 1998. Glacigenic debris flows on the
834 North Sea Trough Mouth Fan during ice stream maxima. *Marine Geology* 152, 217-246.

835 King, E.L., Sejrup, H.P., Haflidason, H., Elverhøi, A., Aarseth, I., 1996. Quaternary seismic
836 stratigraphy of the North Sea Fan: glacially-fed gravity flow aprons, hemipelagic sediments,
837 and large submarine slides. *Marine Geology* 130, 293-315.

838 Laberg, J.S., Andreassen, K., Vorren, T.O., 2012. Late Cenozoic erosion of the high-latitude
839 southwestern Barents Sea shelf revisited. *Geological Society of America Bulletin* 124, 77-88.

840 Laberg, J.S., Forwick, M., Husum, K., Nielsen, T., 2013. A re-evaluation of the Pleistocene
841 behavior of the Scoresby Sund sector of the Greenland Ice Sheet. *Geology* 41, no. 12, 1231-
842 1234.

843 Laberg, J.S., Guidard, S., Mienert, J., Vorren, T.O., Haflidason, H., Nygård, A., 2007.
844 Morphology and morphogenesis of a high-latitude canyon; the Andøya Canyon, Norwegian
845 Sea. *Marine Geology* 246, 68-85.

846 Laberg, J.S., Stoker, M.S., Dahlgren, K.I.T., Haas, H. d., Haflidason, H., Hjelstuen, B.O.,
847 Nielsen, T., Shannon, P.M., Vorren, T.O., van Weering, T.C.E., Ceramicola, S., 2005a.
848 Cenozoic alongslope processes and sedimentation on the NW European Atlantic margin.
849 *Marine and Petroleum Geology* 22, 1069-1088.

850 Laberg, J.S., Vorren, T.O., 1993. A late Pleistocene submarine slide on the Bear Island
851 Trough Mouth Fan. *Geo-Marine Letters* 13, 227-234.

852 Laberg, J.S., Vorren, T.O., 1995. Late Weichselian submarine debris flow deposits on the
853 Bear Island Trough Mouth Fan. *Marine Geology* 127, 45-72.

854 Laberg, J.S., Vorren, T.O., 1996a. The glacier-fed fan at the mouth of Storfjorden trough,
855 western Barents Sea: a comparative study. *Geologische Rundschau* 85, 338-349.

856 Laberg, J.S., Vorren, T.O., 1996b. The Middle and Late Pleistocene evolution of the Bear
857 Island Trough Mouth Fan. *Global and Planetary Change* 12, 309-330.

858 Laberg, J.S., Vorren, T.O., 2000. The Trænadjupet Slide, offshore Norway – morphology,
859 evacuation and triggering mechanisms. *Marine Geology* 171, 95-114.

860 Laberg, J.S., Vorren, T.O., Dowdeswell, J.A., Kenyon, N.H., Taylor, J., 2000. The Andøya
861 Slide and the Andøya Canyon, north-eastern Norwegian–Greenland Sea. *Marine Geology*
862 162, 259-275.

863 Laberg, J.S., Vorren, T.O., Kenyon, N.H., Ivanov, M., Andersen, E.S., 2005b. A modern
864 canyon-fed sandy turbidite system of the Norwegian Continental Margin. *Norwegian Journal*
865 *of Geology* 85, 267-277.

866 Larter, R.D., Cunningham, A.P., 1993. The depositional pattern and distribution of glacial-
867 interglacial sequences on the Antarctic Peninsula Pacific margin. *Marine Geology* 109, 203-
868 219.

869 Nielsen, T., De Santis, L., Dahlgren, K.I.T., Kuijpers, A., Laberg, J.S., Nygård, A., Praeg, D.,
870 Stoker, M.S., 2005. A comparison of the NW European glaciated margin with other glaciated
871 margins. *Marine and Petroleum Geology* 22, 1149-1183.

872 Ó Cofaigh, C., Taylor, J., Dowdeswell, J.A., Pudsey, C.J., 2003. Palaeo-ice streams, trough
873 mouth fans and high-latitude continental slope sedimentation. *Boreas* 32, 37-55.

874 Oljedirektoratet, 2010. Geofaglig vurdering av petroleumsressursene i havområdene utenfor
875 Lofoten, Vesterålen og Senja, 81 pp., Accessible report on: <http://www.npd.no>. (In
876 Norwegian).

877 Osmundsen, P. T., Redfield, T., 2011. Crustal taper and topography at passive continental
878 margins. *Terra Nova* 23, 349-361.

879 Ottesen, D., Dowdeswell, J.A., Rise, L., 2005. Submarine landforms and the reconstruction of
880 fast-flowing ice streams within a large Quaternary ice sheet: The 2500-km-long Norwegian-
881 Svalbard margin (57°–80°N). *Geological Society of America Bulletin* 117, 1033-1050.

882 Ottesen, D., Stokes, C.R., Rise, L., Olsen, L., 2008. Ice-sheet dynamics and ice streaming
883 along the coastal parts of northern Norway. *Quaternary Science Reviews* 27, 922-940.

884 Piper, D. J., Normark, W. R., 2009. Processes that initiate turbidity currents and their
885 influence on turbidites: a marine geology perspective. *Journal of Sedimentary Research* 79,
886 347-362.

887 Posamentier, H.W., Kolla, V., 2003. Seismic geomorphology and stratigraphy of depositional
888 elements in deep-water settings. *Journal of Sedimentary Research* 73, 367-388.

889 Redfield, T., Osmundsen, P., 2013. The long-term topographic response of a continent
890 adjacent to a hyperextended margin: A case study from Scandinavia. *Geological Society of*
891 *America Bulletin* 125, 184-200.

892 Rebesco, M., Camerlenghi, A., Geletti, R., Canals, M., 2006. Margin architecture reveals the
893 transition to the modern Antarctic ice sheet ca. 3 Ma. *Geology* 34, 301-304.

894 Rise, L., Bellec, V.K., Bøe, R., Thorsnes, T., 2009. The Lofoten – Vesterålen continental
895 margin, North Norway: Canyons and mass-movement activity. International conference on
896 seafloor mapping for Geohazard assessment, 11-13 May 2009, Ischia, Italy. In: Chiocci, F.L.,
897 Ridente, D., Casalbore, D., Bosman, A. (Eds.), *Rendiconti Online, Societa Geologica Italiana*,
898 *Extended Abstracts* 7, pp. 79-82.

899 Rydningen, T.A., Laberg, J.S., Kolstad, V., submitted. Late Cenozoic evolution of high-
900 gradient Trough Mouth Fans and canyons on the glaciated continental margin offshore Troms,
901 northern Norway – palaeoclimatic implications and sediment yield. Geological Society of
902 America Bulletin.

903 Rydningen, T.A., Vorren, T.O., Laberg, J.S., Kolstad, V., 2013. The marine-based NW
904 Fennoscandian ice sheet: glacial and deglacial dynamics as reconstructed from submarine
905 landforms. *Quaternary Science Reviews* 68, 126-141.

906 Sejrup, H.P., Hjelstuen, B.O., Dahlgren, K.I.T., Haflidason, H., Kuijpers, A., Nygård, A.,
907 Praeg, D., Stoker, M.S., Vorren, T.O., 2005. Pleistocene glacial history of the NW European
908 continental margin. *Marine and Petroleum Geology* 22, 1111-1129.

909 Sejrup, H.P., King, E.L., Aarseth, I., Haflidason, H., Elverhøi, A., 1996. Quaternary erosion
910 and depositional processes: western Norwegian fjords, Norwegian Channel and North Sea
911 Fan. In: De Batist, M., Jacobs, P. (Eds.), *Geology of Siliclastic Shelf Seas*. Geological
912 Society Special Publication 117, pp. 187-202.

913 Ślubowska-Woldengen, M., Koç, N., Rasmussen, T.L., Klitgaard-Kristensen, D., Hald, M.,
914 Jennings, A.E., 2008. Time-slice reconstructions of ocean circulation changes on the
915 continental shelf in the Nordic and Barents Seas during the last 16,000 cal yr B.P. *Quaternary
916 Science Reviews* 27, 1476-1492.

917 Taylor, J., Dowdeswell, J.A., Kenyon, N.H., 2000. Canyons and late Quaternary
918 sedimentation on the North Norwegian margin. *Marine Geology* 166, 1-9.

919 Tomlinson, J.S., Pudsey, C.J., Livermore, R.A., Larter, R.D., Barker, P.F., 1992. Long-range
920 sidescan sonar (GLORIA) survey of the Antarctic Peninsula Pacific margin. *Recent Progress*

921 in Antarctic Earth Science. In: Yoshida, Y., Kaminuma, K., Shiraishi, K. (Eds.), Proceedings
922 6th International Symposium Antarctic Earth Science. Tokyo, pp. 423-429.

923 Vanneste, M., Berndt, C., Laberg, J.S., Mienert, J., 2007. On the origin of large shelf
924 embayments on glaciated margins – effects of lateral ice flux variations and glacio-dynamics
925 west of Svalbard. *Quaternary Science Reviews* 26, 2406-2419.

926 Vanneste, M., Mienert, J., Bünz, S., 2006. The Hinlopen Slide: A giant, submarine slope
927 failure on the northern Svalbard margin, Arctic Ocean. *Earth and Planetary Science Letters*
928 245, 373-388.

929 Vogt, P.R., Crane, K., Sundvor, E., 1993. Glacigenic mudflows on the Bear Island Submarine
930 Fan. *EOS, Transactions American Geophysical Union* 74, 449, 452-453.

931 Vorren, T.O., Hald, M., Lebesbye, E., 1988. Late Cenozoic environments in the Barents Sea.
932 *Paleoceanography* 3, 601-612.

933 Vorren, T.O., Hald, M., Thomsen, E., 1984. Quaternary sediments and environments on the
934 continental shelf off northern Norway. *Marine Geology* 57, 229-257.

935 Vorren, T.O., Laberg, J.S., 1997. Trough mouth fans – palaeoclimate and ice-sheet monitors.
936 *Quaternary Science Reviews* 16, 865-881.

937 Vorren, T.O., Laberg, J.S., Blaume, F., Dowdeswell, J.A., Kenyon, N.H., Mienert, J.,
938 Rumohr, J., Werner, F., 1998. The Norwegian-Greenland Sea continental margins:
939 Morphology and late Quaternary sedimentary processes and environment. *Quaternary Science*
940 *Reviews* 17, 273-302.

941 Vorren, T.O., Lebesbye, E., Andreassen, K., Larsen, K.-B., 1989. Glacigenic sediments on a
942 passive continental margin as exemplified by the Barents Sea. *Marine Geology* 85, 251-272.

- 943 Vorren, T.O., Plassen, L., 2002. Deglaciation and palaeoclimate of the Andfjord-Vågsfjord
944 area, North Norway. *Boreas* 31, 97-125.
- 945 Vorren, T.O., Rydningen, T.A., Baeten, N.J., Laberg, J.S., 2015. Chronology and extent of the
946 Lofoten-Vesterålen sector of the Scandinavian Ice Sheet from 26 to 16 cal. Ka BP. *Boreas*,
947 10.1111/bor.12118. ISSN 0300-9483.